SAND REPORT
SANDN2002-1925
Unlimited Release
Printed June, 2002

Massively Parallel Global Climate Model for Paleoclimate Applications

Mark B.E. Boslough

Prepared by
Sandia National Laboratories
Albuquerque, New Mexico 87185 and Livermore, California 94550

Sandia is a multiprogram laboratory operated by Sandia Corporation, a Lockheed Martin Company, for the United States Department of Energy under Contract DE-AC04-94AL85000.

Approved for public release; further dissemination unlimited.

Sandia National Laboratories

Issued by Sandia National Laboratories, operated for the United States Department of Energy by Sandia Corporation.

NOTICE: This report was prepared as an account of work sponsored by an agency of the United States Government. Neither the United States Government, nor any agency thereof, nor any of their employees, nor any of their contractors, subcontractors, or their employees, make any warranty, express or implied, or assume any legal liability or responsibility for the accuracy, completeness, or usefulness of any information, apparatus, product, or process disclosed, or represent that its use would not infringe privately owned rights. Reference herein to any specific commercial product, process, or service by trade name, trademark, manufacturer, or otherwise, does not necessarily constitute or imply its endorsement, recommendation, or favoring by the United States Government, any agency thereof, or any of their contractors or subcontractors. The views and opinions expressed herein do not necessarily state or reflect those of the United States Government, any agency thereof, or any of their contractors.

Printed in the United States of America. This report has been reproduced directly from the best available copy.

Available to DOE and DOE contractors from
U.S. Department of Energy
Office of Scientific and Technical Information
P.O. Box 62
Oak Ridge, TN 37831

Telephone: (865)576-8401
Facsimile: (865)576-5728
E-Mail: reports@adonis.osti.gov
Online ordering: http://www.doe.gov/bridge

Available to the public from
U.S. Department of Commerce
National Technical Information Service
5285 Port Royal Rd
Springfield, VA 22161

Telephone: (800)553-6847
Facsimile: (703)605-6900
E-Mail: orders@ntis.fedworld.gov
Online order: http://www.ntis.gov/ordering.htm

SAND2002-1925
Specified Release
Printed June 2002

Massively Parallel Global Climate Model for Paleoclimate Applications

Mark B.E. Boslough
Computational Biology and Evolutionary Computing Department
Sandia National Laboratories
P.O. Box 5800
Albuquerque, NM 87185-0318

ABSTRACT

GENESIS Version 2.0 is a general circulation model developed at the National Center for Atmospheric Research (NCAR) and is the principal code that is used by paleoclimatologists to model climate at various times throughout Earth's history. The primary result of this LDRD project has been the development of a distributed-memory parallel version of GENESIS, leading to a significant performance enhancement on commodity-based, large-scale computing platforms like the CPlant. The shared-memory directives of the original version were replaced by MPI calls in the new version of GENESIS. This was accomplished by means of parallel decomposition over latitude strip domains. The code achieved a parallel speedup of four times that of the shared-memory parallel version at R15 resolution. T106 resolution runs 20 times faster than the NCAR serial version on 20 nodes of the CPlant. As part of the project, GENESIS was used to model the climatic effects of an orbiting debris ring due to a large planetary impact event.

EXECUTIVE SUMMARY

GENESIS Version 2.0 is a general circulation model developed at the National Center for Atmospheric Research (NCAR) and is the principal code that is used by paleoclimatologists to model climate at various times throughout Earth's history. The primary result of this LDRD project has been the development of a distributed-memory parallel version of GENESIS, leading to a significant performance enhancement on commodity-based, large-scale computing platforms like the CPlant. The shared-memory directives of the original version were replaced by MPI calls in the new version of GENESIS. This was accomplished by means of parallel decomposition over latitude strip domains. The code achieved a parallel speedup of four times that of the shared-memory parallel version at R15 resolution. T106 resolution runs 20 times faster than the NCAR serial version on 20 nodes of the CPlant. As part of the project, GENESIS was used to model the climatic effects of an orbiting debris ring due to a large planetary impact event.

ACKNOWLEDGMENTS

Terry Guilinger provided insight and help during the code parallelization phase of this project. Peter Fawcett supplied the paleoclimatology expertise without which the code output could not be interpreted. Dave Pollard was very generous in explaining and helping with his code. Funding was provided under the LDRD program, project 10318, task 01.

CONTENTS **Page**

ABSTRACT 3
EXECUTIVE SUMMARY 4
ACKNOWLEDGMENTS 5
CONTENTS 6
I. INTRODUCTION 7
II. PROJECT OVERVIEW 7
A. Paleoclimatology 8
B. Description of GENESIS 8
III. MODIFICATIONS AND PERFORMANCE 9
A. Parallel decomposition 10
B. CPlant performance 10
IV. APPLICATIONS 11
V. FUTURE WORK 12
VI. REFERENCES 13
APPENDIX A: Climate Effects of an Impact Induced Equatorial Debris Ring
APPENDIX B: Impact-Induced Climate Change Due to an Orbiting Debris Ring
DISTRIBUTION

I. INTRODUCTION

The Third Assessment Report (2001) of the Intergovernmental Panel on Climate Change (IPCC) concluded that "An increasing body of observations gives a collective picture of a warming world and other changes in the climate system." Such climate changes are widely recognized as a potential national security issue, and have been identified by the Department of Energy as important to decision making in many areas relating to stewardship of the planet. The DOE has sponsored climate prediction research since the 1970s, with emphasis on computational simulations and with the goal of improving understanding and prediction of regional and global climate changes. Current DOE climate research programs are focused on codes for modeling present-day climate; to develop, test and apply coupled atmosphere-ocean general circulation models (GCMs) and keep them on the leading edge of science and technology. The latest IPCC report attributed much of our improved understanding of climate change to data from new studies of both present-day climate and *paleoclimate* (pre-historic climate). Because so much of our understanding of climate variability comes from research in Earth system history, it is also important to advance paleoclimate simulation capabilities so that they too take advantage of current high-end computational architectures. The lack of dedicated computational resources within the paleoclimate community has been a major limitation to advancement of that field. The principal paleoclimate code, GENESIS, was not written to take advantage of the increasing availability of massively parallel computers. The development of an MPI version of GENESIS is intended to allow paleoclimate researchers to make better use of current and future computational resources.

II. PROJECT OVERVIEW

The primary purpose of the project was to develop an MPI version of the paleoclimate code GENESIS, leading to significant parallel speedup on machines with MPP architectures such as the CPlant. Auxiliary goals were to develop collaborations in the paleoclimate community, and to simulate and interpret the effects of a ring-producing planetary impact. Recent NRC reports (1998, 2001) have noted with concern that the United States lags behind other countries in its ability to model long-term climate change. In 1998, the NRC found that "insufficient human and computational resources are being devoted to high-end, computer intensive, comprehensive modeling..." The 2001 NRC report pointed out that U.S. climate modeling is still lagging in its ability to produce accurate high-resolution model runs, and that the situation has deteriorated since the 1998 report was published. In particular, the NRC report committee criticized the trade restrictions on import of large vector computers and the *de facto* transition to MPP architectures for climate models that were written and optimized for vector architectures. This transition has lead to a tremendous strain on human resources, due to a shortage of experienced atmospheric scientists and software engineers capable of writing new code for MPP machines. Moreover, most of the effort in retooling at NCAR and the national labs has been the development of codes that are primarily used for modern climate studies, and conversion of specialized paleoclimate codes has not received the same level of attention. Because most major climate modeling centers in the US are now acquiring high-end MPP machines and decommissioning their vector machines, it is important to retool the paleoclimate codes as well. We have chosen GENESIS for this project, because it is the most widely used code for paleoclimate modeling, there is a large

archive of GENESIS research simulation runs, and the paleoclimate community understands and trusts the code.

A. Paleoclimatology

Paleoclimatology is the study of the climate of Earth's prehistoric past. The geologic record contains a detailed paleoclimatic history, demonstrating that Earth's climate is constantly changing over timescales of decades, centuries, and millennia. Climate patterns can be inferred from studies of tree rings, lake sediments, ice cores from Greenland and Antarctica, and stable isotope analyses of marine sediments. These data sets span centuries to millions of years, and reveal a pattern of prehistoric climate that shows a high degree of natural variability, with episodes of sudden change. Understanding the nature of such past climate change is a key element in making sense of current and future climate variability, and allowing computer simulation models to be validated and improved. These climate models are the primary means of integrating our understanding about the physics and dynamics of climate systems, distinguishing between human-caused climate change and natural variability, and predicting how climate is likely to change in the near and distant future.

When the present climate is examined in the context of paleoclimate data, it is apparent that our current environment is anomalous, in that it has been much warmer and more stable over the past 10,000 years than is typical. The Earth has a tendency to be much colder than it is now. There are no accurate temperature measurements before about 1870, but oxygen isotopes studies show that prior to about 7000 BC, temperatures were highly variable. Paleoclimate simulations of this unstable period of Earth's climate history are necessary to generate the understanding needed to assess the likelihood of the return of such instability due to human-induced atmospheric perturbations.

B. Description of Genesis

The GENESIS (Global Environmental and Ecological Simulation of Interactive Systems) code is was developed at the National Center for Atmospheric Research (NCAR) between 1989 and 1997. It was designed for use in both paleoclimate and future climate change research. One of the primary motivations for developing GENESIS was to simulate global climate change due to human causes, including greenhouse gas emissions and changing land use. The original model (version 1.02) is described by Thompson and Pollard [1995], and was used extensively in the early 1990s for paleoclimate, present-day, and future climate applications. The current model (version 2.0) consists of a 3 dimensional atmospheric general circulation model (AGCM) with coupled ocean, vegetation, soil, snow, ice sheets, and sea ice. The AGCM originated from the NCAR Community Climate Model [Williamson et al., 1987], and includes detailed radiative transport calculations for solar and infrared radiation, and parameterized treatments of clouds and precipitation. It makes use of the spectral transform method to integrate horizontal transport of mass, momentum, and energy, and uses the sigma coordinate system in which $\sigma=0$ at the top of the atmosphere, and $\sigma=1$ at the surface, with semi-Lagrangian vertical transport.

The atmosphere and ocean models incorporate large-scale dynamics and convection, and the ocean can be modeled either with prescribed surface temperatures or with slab diffusion. Various models include atmospheric chemistry, ocean biogeochemical cycles, soil microbial and trace-gas activity, climate-induced changes in vegetation, and orbital forcing of solar insolation (Milankovitch forcing). The code consists of tens of thousands of lines of FORTRAN, with 238

subroutines in 16 modules. The original means of parallel execution made use of 18 DOACROSS directives for shared memory architectures. Our parallel performance analysis demonstrated that this code did not exhibit significant speedup beyond a few processors. This version of GENESIS was unable to take full advantage of massively parallel architectures that were increasingly becoming available. The main purpose of this project was to develop a distributed-memory parallel version of the code to significantly improve its performance, enabling researchers to run it at higher resolutions, and for longer simulated time.

In Figure 1, the limited parallel performance of the original version is plotted for various resolutions, measured by the spectral truncation limit (R15 and T31). The first truncation limit refers to the atmospheric GCM, and the second one to the surface model, where "2x2" refers to 2-degree surface gridding. The serial component of GENESIS was roughly estimated by subtracting the 2-processor computation time from the serial computation time. With 22% of time spent on serial tasks, even "perfect speedup" of the remainder would not be worth pursuing. Fortunately, most of the serial parts of this version of the code could also be parallelized.

III. MODIFICATIONS AND PERFORMANCE

With the decreasing availability and higher cost of large vector machines, many climate codes that were developed in the 1980s and 1990s cannot be run by the average researcher on the

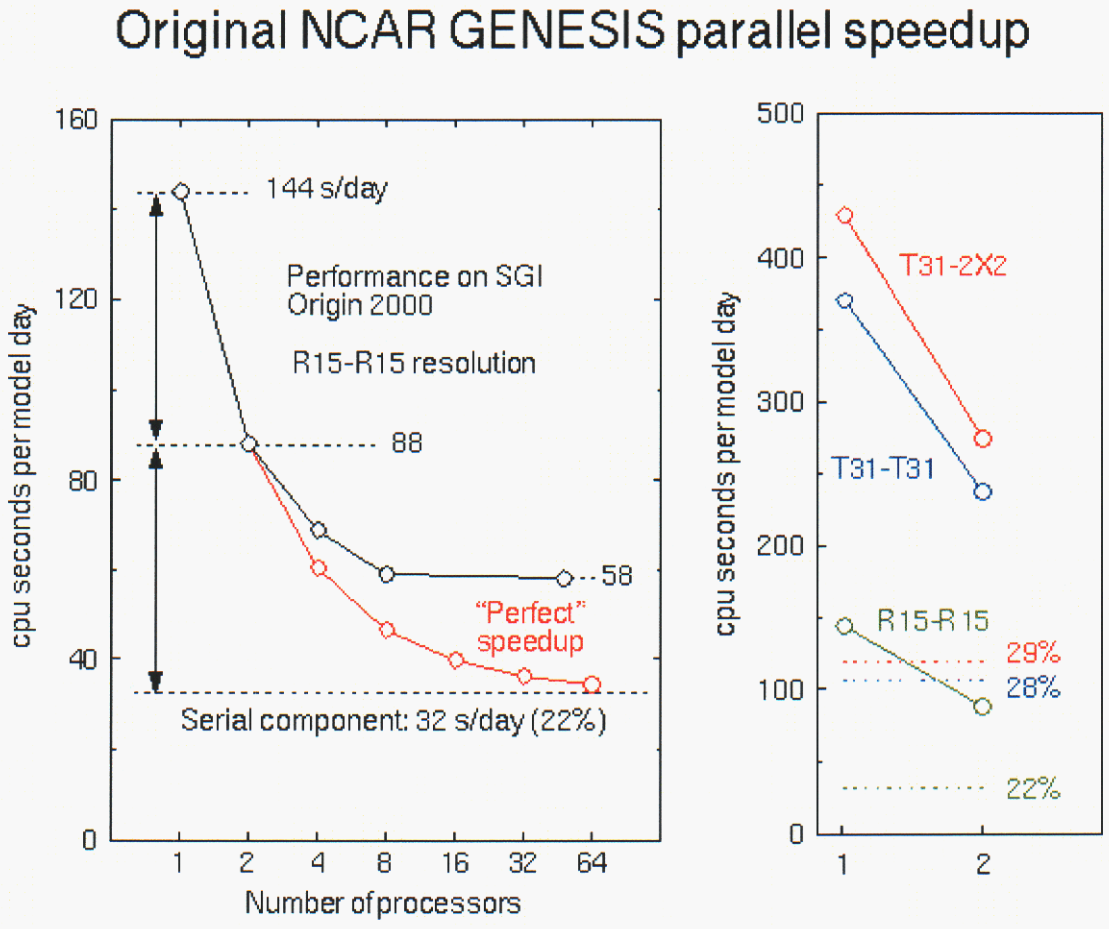

Figure 1. Performance of NCAR shared-memory version of GENESIS.

types of architectures for which they were written. As more and more institutions purchase larger and larger MPP machines, workers that do not have MPP versions of their code are becoming handicapped. One alternative would be to write new codes from scratch, but there is a legacy of simulation and research with existing climate models, which are often used for comparative studies. These codes have been carefully tuned over the years, and the research community has grown to trust them and to recognize their strengths, quirks, and limitations. GENESIS is one such code. Because it is a spectral transform code, there is a transform at each time step between grid space and spectral space, so significant communication between nodes is required. For the most appropriate parallel decomposition, this communication can be minimized, leading to significant speedup on large numbers of processors.

A. Parallel Decomposition

To minimize communication in the MPI version, the grid space was decomposed into latitude domains (Figure 2). General circulation models that use the spectral transform method perform physics calculations (*e.g.* cloud parameterizations, surface interactions, and radiative transport) in grid space, and information remains local. Therefore during the physics calculation no data needs to be exchanged among nodes, except when it is necessary to gather global budget information for various quantities. Physical quantities are smoothed with a cubic spline operator, so information must also be exchanged between two pairs of "ghost strips" before transforming to the spectral domain. The spectral transform is communication-intensive. By exchanging data among processes as illustrated in Figure 2, the Legendre transform computation can be performed on a single processor by having data local. However, the single communication step shown in Figure 2 begins to dominate at high resolution. This is the essence of the lack of scalability of spectral methods for climate modeling at ultra-high resolution.

B. CPlant performance

The MPI version of GENESIS exhibits significant improvement, reaching 21 times the speed of the serial version, and four times the speed of the shared-memory version. The CPlant can now achieve nearly 14 model years per CPU day at T31 (spectral truncation limit) resolution. Typical paleoclimate model runs of 20-30 years can now be performed in a couple of days. This compares to 3 model years/day with the old version of GENESIS for the Cray SV1 at Penn State, and gives us a version with which production runs can be performed. Parallelizing over spectral coefficient further enhanced the performance of the code. This version of the code performs sums as MPI reduction operations during the spectral domain portion of the computation, greatly reducing the communication required every time step, especially for high-resolution simulations.

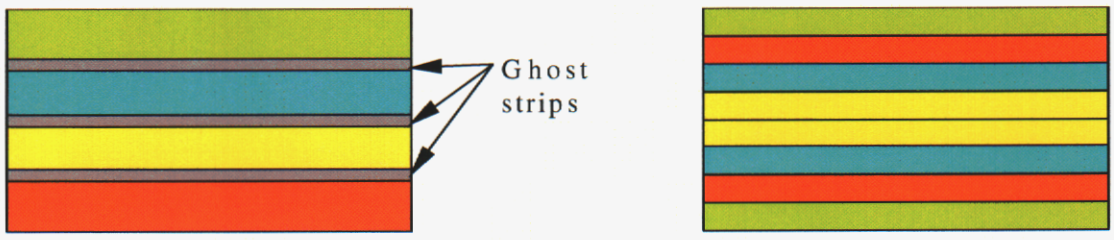

Figure 2. Grid-space decomposition on CPlant; each color represents a processor.

IV. APPLICATIONS

For the modeling part of this project, we used the code to investigate the climatological consequences of the formation of an equatorial debris ring by a large grazing asteroid or comet impact. Several theoretical and laboratory studies suggest that some large impact events are capable of inserting material into space depending on mechanics of the impact. This material would quickly coalesce to form a temporary debris ring in orbit around the equator, which would cast its shadow on the winter hemisphere. Our simulation, where an orbiting equatorial debris ring is applied as a boundary condition to the model, shows how the longer-term effects of a major impact could affect the climate system. The primary effect is a severe cooling in the tropics and the subtropics, especially under the seasonally migrating ring shadow. The globe cools and becomes drier, with the exception of monsoonal regions that become wetter. The Hadley Cell is weakened resulting in drier tropics and weaker subtropical high-pressure cells in the winter hemisphere. Because the tropics cool more than middle latitude regions, the equator-to-pole temperature gradient becomes shallower resulting in weaker tropospheric winds and less high-latitude storminess. We suggest that the late Eocene impact(s) (35.5 Ma) could have generated a geologically temporary orbiting debris ring based on the global distribution of tektites associated with these events and patterns of climate change immediately above the

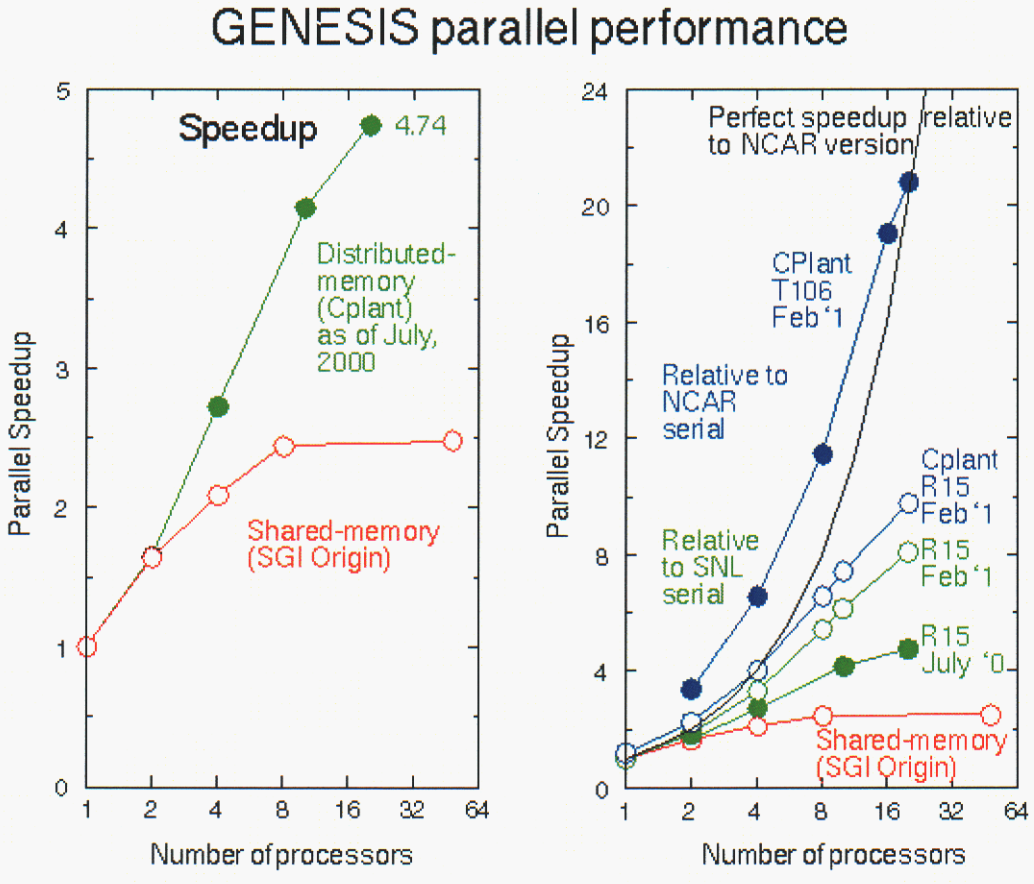

Figure 3. Timing of various versions of GENESIS relative to NCAR release.

iridium/microtektite layer. The Cretaceous-Tertiary boundary event, while larger, did not produce a debris ring. We also suggest that an opaque debris ring could have acted as the trigger to at least one episode of global glaciation during the Neoproterozoic. These results have been prepared for publication, and are attached as Appendix A [Fawcett and Boslough, 2002], and Appendix B [Boslough, 2001].

V. FUTURE WORK

We also identified areas for future improvements, including the re-dimensioning of all global arrays so that only memory that is used is actually allocated. This will decrease latency time for communication as well as pipelining during do-loops. We can also speed up the communication associated with the spectral transform by another factor of two. If the paleoclimate community needs higher-resolution simulations, we can do our parallel decomposition over longitude in addition to latitude. At this stage, using efficient parallel FFT libraries can enhance the performance. The latest parallel version of GENESIS now has the option of running at T63 and T106 resolutions, for which the new distributed memory parallelism has the greatest speedup due to its higher computation/communication ratio.

VI. REFERENCES

Boslough, M.B.E. (2001), "Impact-Induced Climate Change due to an Orbiting Debris Ring," 20th Annual Int. Space Dev. Conf, ASCE, SAND2001-1710C.

Fawcett, P.J., and Boslough, M.B.E. (2002), "Climatic Effects of an Impact Induced Equatorial Debris Ring," *J. Geophys. Res. Atmospheres,* in press, SAND2001-2464.

National Research Council (1998), *Capacity of U.S. Climate Modeling to Support Climate Change Assessment Activities*, National Academy Press, Washington, D.C., 65 pp.

National Research Council (2000), *Improving the Effectiveness of U.S. Climate Modeling*, National Academy Press, Washington, D.C., 128 pp.

Thompson, S.L., and Pollard, D. (1995), "A Global Climate Model (GENESIS) with a Land-Surface Transfer Scheme (LSX). Part I: Present Climate Simulation," *Journal of Climate*, 8, 732-761.

Williamson, D.L., Kiehl, J.T., Ramanthan, V., Dickinson, R.E. and Hack, J.J. (1987), *Description of NCAR Community Climate Model (CCM1).* NCAR Technical Note NCAR/TN-285+STR, Boulder, Colorado, 112 pp.

Appendix A

Fawcett, P.J., and Boslough, M.B.E. (2002), "Climatic Effects of an Impact Induced Equatorial Debris Ring," J. Geophys. Res. Atmospheres, in press, SAND2001-2464.

Climatic Effects of an Impact Induced Equatorial Debris Ring

Peter J. Fawcett

University of New Mexico
220 Northrop Hall
Albuquerque, NM 87131

and

Mark B.E. Boslough
P.O. Box 5800
Mail Stop 0318
Sandia National Laboratories
Albuquerque, NM 87185-0318

Abstract

Several theoretical and laboratory studies suggest that some large impact events are capable of inserting material into space depending on mechanics of the impact. This material would quickly coalesce to form a temporary debris ring in orbit around the equator, which would cast its shadow on the winter hemisphere. The results of an atmospheric GCM simulation where an orbiting equatorial debris ring is applied as a boundary condition to the model show how the longer-term effects of a major impact could affect the climate system. The primary effect is a severe cooling in the tropics and the subtropics, especially under the seasonally migrating ring shadow. The globe cools and becomes drier, with the exception of monsoonal regions that become wetter. The Hadley Cell is weakened resulting in drier tropics and weaker subtropical high pressure cells in the winter hemisphere. Because the tropics cool more than middle latitude regions, the equator-to-pole temperature gradient becomes shallower resulting in weaker tropospheric winds and less high-latitude storminess. We suggest that the late Eocene impact(s) (35.5 Ma) could have generated a geologically temporary orbiting debris ring based on the global distribution of tektites associated with these events and patterns of climate change immediately above the iridium/microtektite layer. The Cretaceous-Tertiary boundary event, while larger, did not produce a debris ring. We also suggest that an opaque debris ring could have acted as the trigger to at least one episode of global glaciation during the Neoproterozoic.

Introduction

A growing body of evidence shows that the Earth has been subjected to numerous impacts by comets and asteroids throughout its history. Notable examples include Meteor Crater, Arizona, the buried Cretaceous/Tertiary Chixulub crater (Hildebrand et al., 1991), a late Triassic chain of at least 5 coeval craters spread across several continents (Spray et al., 1998), the Precambrian Sudbury basin and many more. The effects of the larger impact events on Earth's environment and climate have been the subjects of much speculation and research over the past two decades; much of it focused on the K/T boundary event. Proposed mechanisms for impact-related climate changes include aspects of atmospheric chemistry, aerosol production, and shock heating of the atmosphere (e.g., Prinn and Fegley, 1987; D'Hondt et al., 1994) or a stratospheric dust cloud that blocks a significant fraction of insolation (e.g. Covey et al., 1990; 1994; Pollack et al., 1983; Toon et al., 1982; 1997). Both classes of effects are usually thought to be geologically transient and conditions rapidly returned to pre-impact conditions.

An alternative mechanism to be explored here is an impact generated, circum-equatorial debris ring. Such a ring would enhance and prolong the effects of a large impact on the climate system by casting a shadow in the winter hemisphere of the planet and greatly reducing subtropical insolation receipt. We examine the effects on climate of such a ring shadow with an atmospheric general circulation model. As a first and rather extreme sensitivity test, we use a fully opaque debris ring. This analysis can help to guide interpretation of the geologic record in the absence of a definitive oblique impact crater.

The idea of a circum-equatorial orbiting ring affecting Earth's climate is not new, but has not been widely discussed in the literature. Crowell (1983) suggested that during

times of low-latitude glaciations (e.g., the Neoproterozoic), the Earth might have had an ice ring similar to Saturn's, which blocked equatorial insolation. This idea has not received much credence, as it is unclear how an ice ring could form about the Earth and the intensity of radiation at the Earth's relatively close distance to the sun would quickly ablate the ring away. O'Keefe (1980a) suggested that a temporary Earth ring lasting between one and several million years and made of tektite material could explain the large climatic changes that occurred at the end of the Eocene. This idea was supported by the approximate co-incidence in timing of a large tektite strewn field (Glass and Zwart, 1979) and botanical data that suggest a dramatic decrease in winter temperatures with little change in summer temperatures (Wolfe, 1978). An equatorial ring would cast a shadow on the winter hemisphere and explain the observed pattern of cooling in the biological data. The tektites were assumed to be of cosmic origin, perhaps from lunar volcanoes (see King, 1980 and O'Keefe, 1980b) some of which struck the Earth and some of which missed the Earth and were trapped in geocentric orbit. King (1980) challenged this idea because of a lack of known lunar rocks that are chemically suitable source materials for the tektites and suggested instead that these tektites are more similar in composition to North American tuffs and tuffaceous sediments of this age (i.e. probably produced by an impact event at the Eocene). O'Keefe (1985) has also suggested a tektite ring for the terminal Cretaceous event with the tektite material being derived from lunar volcanic eruptions. Clearly the evidence accumulated since 1985 are much more supportive of a large impact at the K-T boundary.

The tektite strewn fields are now generally considered to be material that has been ejected by bolide impacts (e.g., Koeberl et al., 1996) and traveled through the atmosphere

and possibly in orbit about the Earth. We therefore consider that if the Earth ever did have one or more episodes of a transient circum-equatorial ring, the most likely source of material for the ring is from a large bolide impact. Schultz and Gault (1990) suggested that such an event is possible given a low angle impact and a large enough impactor. Other work has suggested that ejection of impact debris into orbit is possible through hydrodynamic interactions (e.g. Boslough and Crawford, 1997; Crawford et al., 1995).

Impact Events in the Geological Record

The record of large impacts on Earth is rather poorly preserved owing to plate tectonic activity (subduction) and erosion (McLaren and Goodfellow, 1990), subsequent burial of an impact crater by younger sediments (e.g. the K/T boundary Chixulub structure, Hildebrand et al., 1991), and tectonic deformation (e.g. the Proterozoic Sudbury ring structure; Melosh, 1989). Despite this, there are a few exceptionally well preserved impact structures found in the geological record. The most famous of these events is the Cretaceous – Tertiary boundary event that is associated with a major biological extinction. The diameter of the impacting body was estimated to be 10 km based on the global extent of the iridium-bearing clay layer (Alvarez et al., 1980). The actual crater site was discovered at Chicxculub, a 180 km diameter buried bowl structure in the Yucatan Peninsula, Mexico (Hildebrande et al., 1991). Evidence of other large impacts is found throughout Earth history and some examples include a multiple impact event in the late Triassic (Spray et al., 1998), the end of the Eocene (Ganapathy, 1984) and in the Pliocene (Schultz et al., 1998).

Rates of impact events through geologic time have been estimated from a variety of data. The cratering record of the other inner planets and the moon show that the early period of heavy bombardment ended around 3.8 Ga (e.g. Barlow, 1990) and that since then, large impacts have been less frequent. Estimates of impact rates in the Phanerozoic based on the Earth's cratering record and the number of asteroids and comets in Earth crossing orbits (Shoemaker et al. 1988) range from one every 7 to 14 Myr for bolides with a diameter $\geq$ 5 km and one every 55 to 100 Myr for 10 km diameter bolides (Shoemaker, 1983; McLaren and Goodfellow, 1990).

Clearly, large impacts must have affected the evolution of the Earth, life on it, and its atmospheric environment. Most work on the environmental effects of a large impact has been done for the K/T boundary event. A variety of studies suggest that ejection of material from the impact site into the atmosphere will result in the suspension of fine dust in the upper atmosphere blocking a significant fraction of sunlight (Toon et al., 1982; Pollack et al., 1983). The climatic effects of such a stratospheric dust cloud have been investigated by Covey et al. (1990), Covey et al. (1994) and Toon et al. (1997). The collective results of this work suggest an intense global cooling but not a global freeze event. Longer-term effects of large impacts are relatively unknown but some authors have suggested that they could cause tectonic and volcanic episodes (e.g., Seyfert and Sirkin, 1979; Rampino and Stothers, 1988).

Planetary Ring Formation via a (Low Angle) Impact Mechanism

A growing body of evidence and experimental work suggests that large impact events are capable of ejecting some fraction of material into space, which could coalesce

and form a geologically temporary debris ring. The global extent of the iridium-bearing clay layer and shocked quartz at the K/T boundary clearly demonstrates that material was ejected at near-orbital escape velocities following the impact event. A purely ballistic ejection that does not involve hydrodynamic interactions would not allow such particles to remain in orbit, and they would reenter the atmosphere and impact within one orbital period. However, hydrodynamic interactions among the solid debris, the atmosphere, and an expanding vapor cloud are increasingly being recognized as an important component of terrestrial impact physics and this could possibly provide the conditions that would lead to orbital trapping of debris.

Theoretical calculations and laboratory experiments both show that under certain impacting conditions, planetary and impactor material can be inserted into orbit and can even escape Earth's gravity field. O'Keefe and Ahrens (1986) performed a series of calculations that showed the formation of high velocity downrange vapor plumes for a range of oblique impact angles and sufficiently high impact velocities. These vapor plumes could be a mechanism for accelerating surface rocks to planetary escape velocities, and were cited as a means of propelling Martian-origin rocks into space and ultimately to Earth (O'Keefe and Ahrens, 1986).

A series of laboratory experiments have also demonstrated the possibility of injecting substantial amounts of material into orbit (Schultz and Gault, 1990). At low impact angles (30^{o} or less from the horizontal), the original impactor disrupts and ricochets downrange at a significant fraction of its incoming velocity. The ricochet component becomes embedded in and accelerated by an expanding vapour cloud. Continued interaction between the solid debris and the turbulent expanding vapor cloud

can potentially provide the non-ballistic force that allows some fraction of the debris to be inserted into orbit. Schultz and Gault (1990) calculated that the optimum conditions for inserting a large mass of material into orbit would be for an oblique impact between 10^{o} and 20^{o} from the horizontal into an ocean or carbonate sediments with an incoming velocity between 15 and 20 km/sec. For a 10-km-diameter body, the oblique impact event described above would be likely once every 300 million years (Schultz and Gault, 1990).

An orbiting cloud of debris will collapse to a single plane within Earth's Roche limit by the same orbital mechanics that led to Saturn's and other planets' ring systems. Dynamical models of the development and evolution of disk formation predict a rapid ring development through collisional dampening (Brahic, 1977). The stable location for such a planetary ring is the Laplacian plane, defined by the total angular momentum of the planetary system. Saturn is a rapidly rotating, low-density gas giant where the equatorial diameter is 10% greater than the polar diameter. For Earth, the mass of the moon competes with the equatorial bulge so the dynamically stable ring plane would lie between the equatorial plane and the lunar orbit plane (which precesses between 18 and 29 degrees from the equatorial plane). For simplicity, we assume as a first approximation that any ring will lie in the equatorial plane.

Planetary Rings and Insolation

An equatorial ring would cast a shadow primarily in the tropics, as is the case for Saturn. The location, surface area and darkness of the ring shadow would have a strong seasonal dependence, resulting in a net insolation reduction in the winter hemisphere (Figure 1). The maximum insolation loss would be during the solstices when the ring

shadow is most extensive. At the equinoxes, the ring would be parallel to the subsolar direction and the shadow would be negligible.

The radial extent and opacity of an equatorial ring would depend on a number of factors making it difficult to specify any one ring geometry and opacity as the most likely. The grain size, total amount, and optical properties of material inserted into orbit via impact would determine the opacity of the ring (for a given radial extent) and the complex orbital mechanics of a planetary ring in a system with one large moon would determine the radial extent of the ring. Given the main purpose of this work, which is to determine the possible first order effects of an equatorial ring system on the Earth's climate, we have chosen to represent the ring as an opaque, scaled Saturn B-ring. Of Saturn's three classical rings, the B-ring is the optically thickest (opaque) and casts a shadow on Saturn's equator. It extends from a minimum radius, r_{min} of 1.53 Saturn radii to a maximum radius, r_{max} of 1.93 Saturn radii (Cuzzi, 1983). Scaling these dimensions to Earth's radius (6378 km) gives an r_{min} of 9758 km and an r_{max} of 12,310 km. The inner edge of the ring would be 3,380 km above the surface and the outer edge 5,932 km above the surface for a total radial ring width of 2552 km. We have assigned an opacity of one to this ring, such that no light passes through it. This is only one of a multitude of possible ring parameters but as a sensitivity test for the effects of a planetary ring shadow on climate, it serves very well.

The normal insolation pattern for an atmospheric general circulation model was modified by calculating the effects of the ring shadow on insolation. The ring itself lies well outside of the atmosphere and does not interact directly with it, so this scheme was relatively easy to implement. As a first approximation for a small solar declination angle

(δ) the ring shadow covers a latitude band from about $\sin^{-1}(r_{min}/r_{earth} * \sin \delta) - \delta$ to $\sin^{-1}(r_{max}/r_{earth} * \sin \delta) - \delta$. Figure 2 shows the annual hemispheric migration of this ring shadow, as well as the latitudinal extent of the shadow at any particular date. The maximum extent of the shadow occurs at the solstices and covers approximately 13 degrees of latitude. On December 21, the southern limit of the shadow occurs at 14.1°N and the northern limit occurs at 26.8°N. At the equinoxes, there is no shadow. The net annual reduction in globally averaged insolation due to this specific ring geometry and opacity is 17.6 W/m2 (324.2 W/m^2 for the ring case vs. 341.8 W/m^2 for the control).

Global Climate Model

The climate model used in this study is GENESIS v.2 (Thompson and Pollard, 1997), an extensively modified version of the National Center for Atmospheric Research (NCAR) Community Climate Model (CCM1). This model (and an earlier version) has been widely used in a variety of modern and paleoclimate studies. The standard version of the model consists of an atmospheric general circulation model (AGCM) coupled to a land surface model (LSX), which consists of multi-layer models of vegetation, soil, snow, and land ice. Sea surface temperatures are computed using a 50-m slab ocean model coupled to the AGCM, which crudely captures the seasonal heat capacity of the surface mixed layer. A thermodynamic sea ice model predicts the extent and thickness of sea ice. Poleward oceanic heat transport is treated as a horizontal diffusion down the gradient of the mixed-layer temperature with the diffusion coefficient depending strongly on the zonal fraction of land vs. water and on the latitude itself (Pollard and Thompson, 1997). This ocean heat flux parameterization is based only on observed estimates and is not a

'flux correction' method, which allows the model to be used for different paleoclimatic applications (Pollard and Thompson, 1997).

Atmospheric variables including mass, heat, and momentum are calculated as a set of spherical harmonics that are truncated at wave number 31 (T31) that is equivalent to a gaussian grid of 3.75° latitude by 3.75° longitude. The surface model was run on an equivalent grid.

The present-day performance of the model is comparable to that of other coarse-grid models with predicted sea-surface temperatures. Reasonable values are predicted for monthly mean surface temperatures and the diurnal range of temperatures, energy fluxes in the atmosphere, jet stream maximum strengths, and the locations of precipitation maxima (Pollard and Thompson, 1997).

Climate Model Results

In this section, we present the main results of the Earth-ring simulation and compare its climatology to a control simulation run with present day boundary conditions. The ring simulation was run for 16 years and did not achieve a full equilibrium state by this time. However, the rate of change of globally average surface temperature decreased to less than 0.1°C per year by year 13 of the run. As we are comparing the gross features of this climatology to the control and the differences are so large (due to the extreme nature of the forcing), these comparisons are significant within the uncertainty of how much sunlight a debris ring would actually block. The results presented are the averages of the last 4 years of both simulations.

The equatorial debris ring has a profound effect on climate because it reflects a significant fraction of tropical insolation back to space before it can interact with the atmosphere. All aspects of Earth's climate are affected by this seasonal loss of insolation including surface and atmospheric temperatures, equator-to-pole temperature gradients, atmospheric circulation patterns, and the hydrological cycle. We do not attempt a complete and comprehensive analysis of this ring climatology; rather we focus on the climatic highlights that have some likelihood of being preserved in the geologic record.

Surface Temperature

The global, annually averaged surface temperature for the ring simulation is 5.4°C, which is 9.5°C colder than the control (14.9°C). The ring shadow is primarily responsible for this cooling, although secondary positive feedbacks within the climate system act to amplify the global cooling. The surface temperature for both the summer and winter seasons (depending on the hemisphere), December, January, February (DJF) and June, July, August (JJA) are shown in Figure 3. In both seasons, the tropical sea-surface temperatures reach a maximum of about 22°C. Tropical landmasses in both seasons average 10 to 15°C and only rise above 20°C in a few localities and there is a marked winter cooling of subtropical landmasses that are under the ring shadow. The interiors of South Africa, Australia, and South America are substantially below freezing in JJA (-15 to -20°C), as is the interior of Saharan North Africa in DJF. The Northern Hemisphere continents are all below freezing in DJF (Fig. 3a) with interior temperatures of -20°C and colder. Only the southernmost coastal areas have winter temperatures above freezing. Eurasia and North America experience cool summers where surface

temperatures do not exceed 20°C. The high Tibetan Plateau has subfreezing JJA temperatures and is therefore frozen year round. In the high latitudes, the 0°C isotherms are displaced equatorward relative to the control in both seasons: the Southern Hemisphere undergoes a larger displacement.

Zonally averaged surface temperatures for DJF and JJA (Figure 4) show that the ring simulation is on average about 8°C colder than the control, and there are latitudinal bands where the temperature differences are much larger. Two of these bands at 15 to 20 degrees N (DJF) and S (JJA) lie under the average positions of the seasonal ring shadows, and two more are at higher latitudes corresponding to the equatorward shift of the 0°C isotherm (and the sea-ice margin). There is a very small sea-ice related peak at 55 degrees N in JJA. The ring simulation has much shallower equator-to-pole surface temperature gradients in the summer hemispheres relative to the control (Fig 4). The meridional temperature gradient from the equator to about 40 degrees latitude is decreased in the winter seasons. Temperature gradients poleward of this point increase and match those of the control simulation. In the subtropics, the local meridional temperature gradients are significantly steeper relative to the control on the equatorial margin of the ring shadow while a relatively flat gradient occurs under the shadow itself (Fig. 4).

The spatial distribution of surface temperature differences between the control and the ring simulations is shown in Figure 5. In DJF, the largest differences occur in Saharan north Africa (up to 40°C), Alaska, and over the north Atlantic at 60 degrees N. The interiors of other northern hemisphere landmasses are all colder by 10°C or more in the ring simulation. In the southern hemisphere, a zone of 10°C difference occurs at 45 degrees S, while the interiors of south Africa, Australia, southern South America and

Antarctica are all 10°C colder than the control. In JJA, the largest surface temperature differences occur in southern hemisphere landmasses (up to 20 to 30°C) and in a zonal band at 50°S latitude. In the northern hemisphere summer, northern Africa, India and the Tibetan Plateau are colder than the control by 10°C (Fig 5a). The interiors of Eurasia and North America are only 5°C cooler than the control in most places, and in eastern Siberia, the ring simulation is actually 5°C warmer than the control.

In both seasons, the oceanic surface temperature differences under the ring shadows are not significantly greater than the surrounding ocean regions except in a few places. This is primarily due to the heat capacity of the ocean model mixed layer, which buffers temperature change at the surface. The model also has a diffusive ocean heat parameterization that advects heat into the shadow region rather quickly, and for this case, probably unrealistically. The surface air temperature differences (not shown), are larger than the surface temperature differences.

Atmospheric Pressure and Circulation Patterns

The patterns of semipermanent and seasonal highs and lows in the ring simulation are grossly similar to the control patterns but their locations are shifted in many cases, and their relative strengths are modified in a complex fashion. The most striking differences are the weakened high-latitude winter lows, the weakened winter subtropical highs, and the strengthened summer continental lows over the major monsoonal regions of the world (Figure 6 and 7). The differences in sea-level pressure between the control and ring simulations (Fig. 7) are difficult to interpret without discussing concurrently the positions and strengths of highs and lows in the ring simulation (Fig. 6). In DJF, the

Aleutian and Icelandic lows are present but are weakened with respect to their control counterparts (core pressures are higher by up to 18 mb and 8 mb respectively, Figs 6a and 7a). The Aleutian Low actually becomes two separate low-pressure centers with one located just east of Japan and the other, deeper low centered over the Alaskan panhandle (Fig 6a). At approximately the same latitude band, the high pressures in the interiors of Eurasia and North America are strengthened relative to the control by 2 to 6 mb (Fig 7a). Winter subtropical high-pressure belts are weakened in the eastern Atlantic and in the eastern Pacific (by up to 8 mb) in the ring simulation. In contrast, the subtropical continental highs present in the control over northern Africa and India are strengthened considerably in the ring simulation (by up to 10 mb over the Sahara). The smaller high over Central America is also strengthened by about 2 mb in the ring simulation. The stronger continental high-pressure zones all lie under the ring shadow. In the Southern Hemisphere, the summer thermal lows over the interiors of south Africa, Australia and South America are deepened by 2 to 4 mb in the ring simulation (Fig 7a) strengthening these small monsoonal circulations. The prominent subpolar zonal low around Antarctica is weakened by 4 to 6 mb.

The JJA sea-level pressure differences between the ring and control simulations are enhanced relative to DJF. Strong thermal lows are developed over all of the major Northern Hemisphere landmasses in the ring simulation (Figure 6b) which results in much stronger summer monsoonal circulations (discussed below). These surface lows are considerably deeper than their control simulation counterparts (pressures are lower by up to 8 mb over northern Africa, 16 mb over the Tibetan Plateau, and 10 mb over SW North America) but are found in approximately the same locations. The Pacific High is

strengthened considerably in the ring simulation and displaced slightly to the north (Figs. 6b and 7b). The Bermuda High is not greatly changed in strength or location, although sea-level pressures are lower by 8 mb in the Azores region. The tropical low-pressure zone is similar in both simulations.

The winter (JJA) highs over the three Southern Hemisphere middle-latitude landmasses are strengthened, while the oceanic subtropical high-pressure zones are weakened by 2 to 4 mb (Figs. 6b and 7b). The circum-Antarctic low-pressure belt is weakened considerably relative to its control counterpart with pressure higher by up to 14 mb (Fig. 7b). The Antarctic high pressure is weakened by up to 8 mb so that this high-latitude land-sea pressure contrast is reduced relative to the control simulation.

Surface Wind Patterns

The large-scale surface wind patterns for DJF and JJA for the ring simulation (Figure 8) are not substantially different from those of the control (not shown) but there are important differences in some aspects of the circulation. In most cases, these are related to the differences in sea-surface temperatures and in sea-level pressure fields between the two simulations. In the tropics and the subtropics, the trade winds on either side of the equator are not significantly strengthened or weakened, but the Intertropical Convergence Zone (I.T.C.Z.) is shifted by a few degrees of latitude into the summer hemisphere.

In JJA, stronger anti-cyclonic flow around the north Pacific high penetrates well into eastern Siberia and stronger northwesterly winds flow along the west coast of North America. A similarly strengthened pattern is seen over the North Atlantic with stronger

winds flowing along the east coast of North America and the northwest coast of Africa (Figure 8a). In this simulation, the Atlantic trade winds do not penetrate into the interior of northern South America while in the control, they do. All of the Northern Hemisphere monsoon regions experience stronger southerly winds and enhanced convergence in JJA relative to the control. The areas most strongly affected are northern Africa, the SW Asia and the Indian subcontinent and SW North America. The low-level Somali Jet is considerably strengthened in the ring simulation, as is the low-level southern plains jet in North America. In the Southern Hemisphere winter, the axis of strong westerlies is shifted south from about 45°S (control) to about 60°S (ring). Cyclonic flows are better developed over the Southern Hemisphere continents (excluding Antarctica) in the ring simulation in response to higher surface pressures under the ring shadow.

In DJF, the westerlies across both the Pacific and the Atlantic Oceans are significantly weaker than in the control. The strong anti-cyclonic circulation in the North Atlantic control simulation is absent in the ring simulation, and the strong anticyclone over Greenland pushes further to the south (Fig. 8b). As in the Southern Hemisphere winter, the winter trade winds at the poleward side of the ring shadow weaken as the trade wind belt shifts south. In the summer hemisphere, summer monsoonal winds are strengthened over south Africa, northern Australia and both east and west central South America. The position and strength of the Southern Hemisphere summer westerlies are not significantly changed relative to the control.

Longitudinally Averaged Zonal Winds

A latitude-pressure (height) cross-section of longitudinally averaged zonal wind is shown in Figure 9 for January and July of both simulations. Important differences occur

in both the summer and winter hemispheres including the strength and locations of the tropospheric westerly jets and of the subtropical easterlies at the tropopause up into the stratosphere.

Two prominent maxima in zonal wind speeds occur in the Southern Hemisphere winter of the ring simulation (July, Fig 9a). One is located at approximately 30°S and occurs as a distinct jet while the other is located at 60°S and occurs as a downward extension of strong westerlies from the stratosphere into the lower troposphere. The core speeds in both the winter and the summer jets are reduced in the ring simulation relative to the control. The summer jet undergoes a larger relative decrease with core wind speeds just above 5 m/sec compared to 15 m/sec in the control.

The most significant new pattern found in the ring simulation is a strong easterly jet that forms in July in the northern hemisphere subtropics. This jet is centered at the tropopause and extends up into the stratosphere (Fig 9a). The stronger subtropical easterlies in the ring simulation extend down through the troposphere to the surface resulting in two distinct features. The easterly belt is widened in the middle troposphere and at the surface, and the surface to lower troposphere zonal winds are stronger than in the control.

The January summer and winter middle latitude westerly jets (Fig 9b) are reduced in strength relative to the control, but both occupy roughly the same positions as their control counterparts. There is no second, poleward zonal wind speed maximum in the Northern Hemisphere in January. In the Southern Hemisphere, subtropical easterlies are stronger in the ring simulation at the tropopause, but no distinct easterly jet is developed

as it is for the Northern Hemisphere summer. The surface to lower troposphere easterlies south of the equator are stronger than in the control.

The Hydrological Cycle

All of the changes discussed so far in temperature fields and atmospheric circulation patterns have a profound effect on the global hydrologic cycle. In this section, we examine changes in precipitation rates and patterns, evaporation rates, and snow cover and sea-ice changes.

Precipitation

All of the major features in modern global precipitation patterns are present in the ring simulation (Figure 10) including the Intertropical Convergence Zone (I.T.C.Z.), the secondary middle latitude precipitation maxima, monsoons, and dry polar winters. However, there are substantial differences with the control both in amounts of precipitation and in some of the spatial patterns of precipitation. Overall, the ring simulation is considerably drier. The global mean annual precipitation rate is 71% of the control value, although it should be noted that the control simulation precipitation rates are higher than observed (Thompson and Pollard, 1997). Zonally averaged precipitation rates for the control and ring simulations are shown in Figure 11 for JJA and DJF. The largest zonal differences occur at the equator and the smallest occur at the poles. A prominent, secondary precipitation maximum on the poleward side of the ring shadow is another unique feature of the ring shadow simulation. While this feature is evident in the winter hemisphere of the zonally averaged precipitation plot (Fig 11), the maxima only

occur over the ocean (Fig 10). Similar secondary precipitation maxima occur in the control simulation (not shown) but they are not as pronounced and are found more in the middle latitude regions.

Precipitation difference plots (Figure 12) show that over most parts of the globe, the control simulation is considerably wetter than the ring simulation. The areas of greatest difference are in the tropics in general and within the I.T.C.Z. specifically where differences can be as large as 12 to 18 mm/day. Precipitation differences are smallest over high latitude regions and mid-latitude land areas in winter. Despite an overall drier global climate in the ring simulation, subtropical monsoon regions are much wetter than in the control. The largest area of enhanced summer precipitation extends from western North Africa across the Arabian Peninsula into the northern part of the Indian subcontinent (Fig. 12a). At the core of this enhanced monsoon region in the ring simulation, precipitation rates are up to 9 mm/day higher than the control (e.g. Saharan North Africa). Southwestern North America and most of northern Mexico also show large positive summer precipitation anomalies relative to the control. Except for one location on the equator, southeast Asia shows a precipitation decrease in the ring simulation in contrast to the other monsoon regions. Areas of non-monsoonal summer precipitation increases include northern China and northeastern North America (Fig. 12a). In the Southern Hemisphere, enhanced summer monsoons occur over south Africa, northern Australia and south-central South America. The maximum difference with the control is just over 3 mm/day in Australia (Fig. 12b). At higher latitudes, a marked decrease in precipitation rates (3 mm/day) occurs in a belt over the oceans centered at 45°S (Fig. 11b, 12b).

Precipitation differences in the winter season of both hemispheres are also significant. In all of the subtropical monsoon regions, negative precipitation anomalies (i.e. wetter in the ring simulation) persist from summer (Fig. 12) suggesting a positive feedback from soil moisture anomalies. Winter precipitation values show a decrease of 1 to 4 mm/day at 40°N latitude in the ring simulation. The largest positive anomalies occur in the eastern Pacific and northwestern North America, the North Atlantic and Europe into central Asia (Fig. 12b). In the Southern Hemisphere, the largest positive anomalies (3 to 4 mm/day) occur in a belt over the southern Ocean centered at 45°S (Figs. 11a, 12a).

Evaporation

In both JJA and DJF, zonally averaged evaporation rates are consistently lower in the ring simulation by 0.25 to 3 mm/day (Figure 13). In this simulation, evaporation rates are highest just poleward of the equator in the winter hemisphere where surface winds are higher. Zonal rates fall rapidly just poleward of these maxima between 15 and 25 degrees of latitude (N or S depending on the season). The largest differences with the control occur in the tropics (roughly between 20°S and 20°N) and there are three distinct difference peaks evident in both seasons (Fig. 13). One peak occurs between 15 and 20 degrees of latitude in the winter hemisphere, corresponding with the seasonal ring shadow. The second peak occurs in the summer hemisphere subtropics (about 15 degrees latitude) where surface winds are weaker in the ring simulation. The third peak occurs in both seasons between 45° and 50°S where evaporation rates are considerably lower in the ring simulation because of a significant poleward advance of sea-ice (next section).

Evaporation rate differences are lower at higher latitudes elsewhere, and are minimized between 20 and 30°N where summer monsoons are stronger in the ring simulation.

Sea-Ice and Snow Cover

The predicted amounts of sea-ice and snow cover for the ring simulation show dramatic increases relative to the control simulation and act as a powerful positive feedback to the global cooling. Both sea-ice extent and snow cover thickness are combined into single plots for JJA and DJF (Figure 14) as the sea-ice margin (not shown) closely corresponds to the snow cover limit over the oceans.

Sea-ice in the Southern Hemisphere winter (JJA, Fig. 14a) extends from the Antarctic coast to about 35°S, a considerable equatorward expansion relative to the control. The Drake Passage is effectively closed to surface ocean circulation and the sea-ice limit also reaches southernmost Australia and New Zealand. Significant amounts of snow cover (> 10 cm thickness) occur over South Africa, Australia and South America where the snow cover extends to 10°S latitude in the Amazon Basin. The areas of thickest snow cover occur over Antarctica and Patagonia. In the Northern Hemisphere summer, the sea-ice margin lies at about 55°N in both the Atlantic and Pacific Oceans. Summer snow cover persists across northern North America, eastern Siberia and northwest Europe as well as over the Tibetan Plateau.

In the opposite season, DJF (Fig. 14b), the Southern Hemisphere sea-ice margin lies at 40°S, still closing the Drake Passage. Summer snows persist in Patagonia, the central Andes, New Zealand and Tasmania, and in southernmost South Africa. The Northern Hemisphere sea-ice front migrates to 50°N and virtually all of the major

landmasses are snow covered. Snow cover reaches to within 10°N of the equator in Saharan north Africa, southern India, southeast Asia, and covers almost all of Mexico. Areas of significant snow depths include the North American cordillera, central to eastern North America, Greenland, the Tibetan Plateau and eastern Siberia. Higher snow depths also occur across Europe.

Discussion

The main goal of this study is to describe the possible long-term effects of large, oblique planetary impact events that are capable of inserting significant quantities of material into orbit. While no definitive case for such an impact has been made from the geologic record, calculated probabilities suggest that over the long span of Earth history several such events must have occurred (e.g. Schultz and Gault, 1990). By using an atmospheric GCM, we have determined the possible climatic effects of a geologically temporary, equatorial debris ring. In all likelihood, Earth would not have experienced the full extent of the climatic effects reported here if a debris ring had formed, because it is unlikely that the ring would be fully opaque. However, these results can guide interpretations of the geologic record where the effects would be similar but not as extreme as depicted here.

Ring Shadow Climatology

The effects of a fully opaque debris ring in orbit around the equator are profound and wide-ranging. Almost all aspects of the simulated climate system are affected by the loss of insolation in the subtropics of the winter hemisphere. The immediate effect of the

ring shadow is a dramatic cooling of the tropical oceans and subtropical landmasses. Directly under the shadow, the ocean does not cool as much as the land due to its greater heat capacity and its ability to advect heat laterally. This lateral advection of heat from the tropics into the subtropical ring shadow region is partly responsible for the tropical cooling and there is much less heat available for export to the middle and high latitudes. At the higher latitudes, snowcover extent increases and the sea-ice margins expand equatorward, acting as a powerful positive feedback to the global cooling. Snowcover persists year round in several high latitude and high altitude locations including the Tibetan Plateau, Patagonia, northern Canada, and the northern fringe of Eurasia (Fig. 14). As discussed earlier, this simulation was close to, but not fully in equilibrium after 16 years (the change in global temperature during the last 4 years of the simulation was less than $0.1^{\circ}C$). We expect that the sea-ice margins would continue their equatorward migration and enhance the global cooling, although it is unlikely that a "snowball Earth" scenario would result with the present day solar constant and atmospheric CO_2 concentrations.

The cooler surface temperatures of the ring shadow simulation significantly reduce evaporation rates, especially in the tropics. The strength of the Hadley Cell circulation is weakened because the cooler tropical sea-surface temperatures promote less deep convection and a lower atmospheric water vapor content. The weakened Hadley circulation reduces the strength of oceanic subtropical highs in the winter hemisphere (Fig. 7). Over winter hemisphere subtropical landmasses, however, stronger high pressure cells are the result of the intense cooling under the ring shadow.

One of the most surprising results of the ring shadow simulation is the tremendous strengthening of summer monsoon winds and rainfall amounts. The area most affected is northern Africa (Figs. 10 and 12), but the other major monsoon regions of the world are also enhanced. This result is not intuitive because the summer hemisphere land surface temperatures are markedly cooler than in the control. As the land-sea thermal contrast is the major driving force for a monsoon circulation, the cooler land surface temperatures alone should promote a weaker monsoon. However, in the ring simulation, the degree of tropical and subtropical ocean cooling is actually larger than in the interiors of the large continents including Asia, northern Africa/Arabia, and North America (Fig. 4). This occurs because the ring shadow in the winter hemisphere draws a massive export of surface ocean heat across the equator from the summer hemisphere into the winter hemisphere. By this process, the ring shadow actually enhances the land-sea thermal contrast in the major monsoon regions of the world. The resulting summer monsoon winds are stronger (e.g. the low-level Kenyan jet, Fig. 8a) and transport more moisture into the interiors of Asia, Africa and North America. Land surface temperatures are still warm enough to promote cumulus convection, and the additional latent heat release from the extra moisture convergence helps to strengthen all of these monsoonal flows. The surface lows in the summer monsoon regions are considerably deeper, and have wider spatial extents in the ring simulation (Figs. 6 and 7). The same process works in the Southern Hemisphere summer (DJF) to strengthen these monsoons (Australian, northern South America) relative to the control, but because the landmasses are smaller, the monsoons are still relatively small.

The presence of stronger monsoon circulations in the ring simulation, especially over Asia and northern Africa, has significant effects on other parts of the climate system. An intense tropical easterly jet forms in the summer near the tropopause above central Asia and accelerates to the east over northern Africa. This jet forms on the equatorward side of a strong, upper level high over Tibet (paired with the deep surface low) where the contrast in temperatures between this region and the air above the ocean to the south produces a strong north-south pressure gradient and easterly winds. Regions affected by the stronger summer monsoons are considerably wetter in the ring shadow simulation and the precipitation anomalies persist into winter (Fig. 12). This is especially evident over north Africa, Arabia, and SW North America where the winter cooling is largest (ring shadow). The cold temperatures severely curtail evaporation rates and promote the buildup of snowcover in the subtropics (Fig. 14).

Tropospheric winds are weakened in the ring simulation, especially the middle-latitude westerly jets (Fig 9). The weakened winds are a direct consequence of the ring shadow blockage of insolation in the tropics, and a shallower equator to pole temperature gradient (Fig. 4). In the winter hemisphere, there is a split in the upper level westerly jet stream, especially in the southern hemisphere (Fig. 9). The second, subtropical jet forms near the strong temperature contrast on the poleward side of the ring shadow.

Winter high-latitude low pressure cells including the Aleutian low, the Icelandic low, and the circum-Antarctic subpolar low are considerably weakened (Figs. 6 and 7). The weakened winter lows imply reduced baroclinic instability in the middle latitudes and fewer and/or weaker winter storms. This appears to be the product of a reduced equator-to-pole temperature difference, and weakened subtropical highs in the winter

hemisphere that weaken atmospheric flow in the middle latitudes. In addition, the winter sea-ice margins are displaced equatorward and this moves the polar front equatorward over the oceans. In the northern summer, the Pacific high is considerably strengthened and is moved poleward in response to the enhanced summer monsoon over North America (cf. Rodwell and Hoskins, 2001). Stronger southeasterly winds around this strengthened high are responsible for the warmer temperatures in eastern Siberia in the ring simulation (Fig. 5) and help maintain the stronger summer monsoon over southeastern Asia.

Predicted Climatic Effects of a Ring Shadow in the Geologic Record

If the Earth ever did have a geologically temporary, orbiting debris ring how would we know? Evidence from the sedimentary record (e.g. Iridium anomalies; Alvarez et al. 1980) correlated with an impact structure is one way to tell if an impact has occurred, and estimates can even be made about the size of the impacting body. This information by itself, however, is not enough to determine if the impact occurred at a sufficiently low angle and with enough energy to insert material into orbit. Based on the climatology of the ring shadow simulation, we can make some essential predictions about what the climate preserved in the geologic record should look like during such an event. Such an analysis is complicated by two factors. First, a debris ring would in all likelihood not be fully opaque and the predictions made here would represent an extreme end-member climate. Second, the transient nature of such a climate perturbation would restrict its stratigraphic record and make global correlations difficult, especially in pre-

Quaternary rocks. However, correlation of climate records from the sedimentary interval just above a global Iridium anomaly would help facilitate such an analysis.

The primary signature of an orbital equatorial debris ring would be a dramatic cooling that persisted over a much longer interval than the immediate effects of a large impact (i.e. the time it would take for a stratospheric dust cloud to dissipate). The cooling would be global, but enhanced in winter. The subtropics should see a larger cooling than surrounding regions, and the cryosphere would expand equatorward. The globe as a whole would be drier; especially in the tropics and so one might look for a shift in vegetation to drier types. The exception to the drier trend is the enhanced summer monsoons, which would increase precipitation in many areas. The magnitude of this effect would depend as much on the continental geometry of the time period (i.e. larger continents promote stronger monsoons) as the opacity of the orbiting debris ring.

The reduced tropospheric wind speeds, especially in the cores of the westerly jets might be reflected in the geologic record as reduced atmospheric dust transport and smaller eolian grain sizes in ocean sediments (cf. Rea et al., 1985). The severely weakened high-latitude winter low pressure cells and fewer/weaker storms would be difficult to discern in the geologic record apart from the resulting lower precipitation rates.

Assessment of the Geological Record

The number of recognized large impacts in the geologic record has increased every year since Alvarez's seminal paper in 1980 but many more will undoubtedly be found in the future. Of the currently known impact events, there are a few potential

candidates for an oblique, high-energy event that might have been capable of inserting material into orbit. In this section we assess the geologic record of climate following a late Eocene impact, the Cretaceous-Tertiary boundary event, and farther back in time during the Neoproterozoic. We suggest that of these events, the late Eocene is the most likely to have produced an orbiting debris ring and that the K-T boundary event did not. We also suggest that the Neoproterozoic "snowball Earth" episodes (Hoffman et al., 1998) could have been started by a large, oblique impact and attendant debris ring.

The late Eocene impact event was initially recognized on the basis of a meteoritic iridium anomaly, which is overlain by a microtektite layer (Ganapathy, 1984). Two very closely spaced (stratigraphically) tektite strewn fields representing impact ejecta are now recognized at this time interval (35.5 Ma), the North American strewn field and the Pacific strewn field. Of the two, the Pacific strewn field is much larger spanning a wide circum-equatorial swath around the globe and it is now recognized at higher latitudes (Vonhof and Smit, 1999). The 100 km diameter Popigai crater in Siberia is a possible source crater for the Pacific strewn field (Vonhof and Smit, 1999) and the North American strewn field has been linked to the Chesapeake Bay impact structure (Koeberl et al., 1996). Wei (1995) suggested that the two major strewn fields were in fact the same event, but no other author has made this claim. Whether these tektite strewn fields represent one or two events, the (near) global distribution of impact ejecta indicates that a large amount of material was accelerated to at least a suborbital trajectory and some fraction of this may have been inserted into orbit.

The climatic record from the sedimentary interval immediately above the iridium/microtektite interval has been studied at two widely separated localities, the

Massignano section in central Italy and at the Maud Rise in the Southern Ocean (Ocean Drilling Project site 689). Both sections show a cooling event of about 2°C with an estimated duration of 100 k.y. (Vonhof et al., 2000). At the Maud Rise, $\delta^{13}C$ data show a surface water productivity increase that is attributed to the cooling. The authors of this study point out that 100 k.y. is too long a cooling to be explained by an impact event alone and suggest a feedback mechanism involving more snow and ice cover maintained the cooler temperatures. We suggest that an orbiting debris ring casting its shadow in the subtropics could have sustained this extended post-impact cooling. The estimated lifetime of such a ring is on the order of 100 k.y. to ~ 1 million years (Schultz and Gault, 1990), similar to the duration of this climatic event. The magnitude of the cooling is much smaller than in the ring shadow simulation, which suggests that if a debris ring was responsible, it was probably not opaque.

O'Keefe (1980a) originally suggested that an orbiting tektite ring (of lunar origin) could explain a major climatic change at the Eocene-Oligocene boundary. Indeed there are many aspects of climate change from the Eocene to the Oligocene that are grossly similar to the ring shadow predictions, and these include a global cooling (e.g. Wolfe, 1978; Zachos et al., 1994) a buildup of ice on Antarctica (e.g. Zachos et al., 1992), a general trend towards drier vegetation types (e.g. Fredericksen, 1988; Oboh et al., 1996), and at the boundary itself, a major extinction of marine invertebrates (Raup and Sepkoski, 1986). Ivany et al. (2000) suggest that winters in the Gulf of Mexico became about 4°C colder with no apparent change in mean annual temperatures across the Eocene-Oligocene boundary. However, a closer examination of these changes at the boundary shows that they are unlikely to have been caused by an orbiting ring. A major

problem is that the boundary occurs about 1.8 million years after the impact events (33.7 Ma vs. 35.5 Ma) so it becomes difficult to attribute cause (impact) and effect (boundary) with such a long lag. The cooling from the Eocene to the Oligocene actually takes place over several million years, and there is no discernable cooling at the boundary in low latitude oceans (Zachos et al., 1994; Ivany et al., 2000). Wolfe (1978) described the cooling from the Eocene to the Oligocene on the basis of vegetation changes, primarily in North America, which O'Keefe attributed to a ring. These vegetation changes occurred over millions of years, however, and are more consistent with a long-term climate change than a single abrupt event. We argue that a debris ring did possibly form during the late Eocene via an impact mechanism and did affect climate in a transient way, but it occurred before the Eocene-Oligocene boundary changes.

The Cretaceous-Tertiary boundary impact was much larger than the late Eocene impact(s) and had a much larger immediate effect on Earth's environment, both in terms of extinctions (Raup and Sepkoski, 1986) and atmospheric perturbations (e.g. Prinn and Fegley, 1987; Sigurdson et al., 1992). Once the immediate effects of the impact dissipated, there were no observed longer-term effects on the climate system. Brinkhuis et al. (1998) report no changes in sea-surface temperatures above the impact horizon and Mukhopadhyay et al. (2001) report lower deep-ocean carbonate sedimentation rates during the ~10 k.y. of the K-T boundary clay deposition and then a return to pre-impact values. The K-T boundary event probably did not generate a planetary debris ring, reinforcing the idea that the geometry of an impact is more important that the size of the impacting body in ring formation.

One of the more interesting climatic episodes in Earth history occurred during the Neoproterozoic when the planet may have undergone a global glaciation or snowball Earth (Hoffman et al., 1998; Kirschvink, 1992). Part of the evidence for a snowball Earth is enigmatic low-latitude glacial deposits that Crowell (1983) suggested could be the result of an equatorial ice ring. Assuming that the Earth had some degree of axial tilt from the ecliptic, a ring will only cast a shadow in the winter hemisphere subtropics and these regions will receive full summer insolation amounts. Based on the ring shadow simulation, the tropics and subtropics are still warm enough in summer to prohibit the formation of low-latitude, sea level glaciers. (However, high elevation areas like Tibet are snow-covered year round.) Therefore, an equatorial ring would not allow glaciers to grow in the tropics to the exclusion of higher latitude regions. We do note, however, that with an opaque ring, the cooling of the tropics allows for an equatorward expansion of snow and ice cover and a positive feedback on the climate system. Given a reduction in solar insolation during the Neoproterozoic (about 5 to 6% lower than today; Endal, 1981) and a sufficiently opaque debris ring, it is possible that a large, oblique impact could act as the trigger sending the Earth into a snowball Earth state. Once the Earth was in a high-albedo frozen state, the ring shadow would become less important and the Earth could remain in a frozen state for millions of years after the ring dissipated. A 150 km diameter impact structure, Acraman, has been found in the Neoproterozoic of Australia (Williams, 1994) and is estimated to have occurred at about 590 Ma which roughly matches the timing of one of the later episode of possible global glaciation (Marinoan ~600 to 575 Ma). We are unaware of any earlier craters so it is difficult to fully evaluate this as a possible mechanism for generating all episodes of Neoproterozoic snowball Earth. There

are other plausible explanations for the onset of a global glaciation (tectonic effects, rapid drawdown of atmospheric CO_2; Hoffman et al., 1998).

Conclusions

Theoretical and laboratory studies suggest that some large impact events are capable of inserting material into orbit depending on the energy and angle of impact. This material would quickly coalesce to form a temporary debris ring in orbit around the equator. The orbiting ring would cast its shadow on the winter hemisphere and could drastically alter the climate system during its lifetime depending on the amount of material and opacity of the ring. The results of our ring shadow simulation with an atmospheric GCM show what kinds of effects could result under such a scenario. As a first order sensitivity test, we chose to use a fully opaque ring, which blocked all insolation under its shadow.

A tremendous cooling in the winter hemisphere subtropics results from the ring shadow, especially over landmasses. The ocean surface cools and rapidly advects heat in from the surrounding ocean due to strong temperature contrasts. This cools the entire tropical ocean, which affects the rest of the climate system. High-latitude regions cool dramatically because of the reduced poleward heat transport from the tropics, especially in the winter hemisphere. Snow cover and sea-ice margins advance towards the equator acting as a powerful positive feedback, cooling the globe even more. The equator-to-pole temperature gradient becomes shallower, especially in summer, which weakens tropospheric winds. Westerly jets are weakened in their core wind speeds, and a second, subtropical jet develops in the winter hemisphere on the equatorward side of the ring

shadow. High-latitude winter lows are considerably weakened due to an overall reduction in baroclinic instability and storminess.

In the tropics, the strength of the Hadley Cell is reduced and the I.T.C.Z. while still present does not have as much rainfall. The subtropical oceanic highs in the winter hemisphere are weakened and this also contributes to the lower tropospheric wind speeds. With the drastic cooling of the tropical and subtropical oceans, subtropical land-ocean temperature contrasts are enhanced and this helps generate much stronger summer monsoons. Areas that are deserts today as well as current monsoonal areas become considerably wetter, and a strong easterly jet forms at the tropopause over central Asia. Everywhere else, the globe is drier because of the cooler sea-surface temperatures and reduced evaporation rates.

Based on this simulation, we made a number of predictions about what the climate record in the geologic column would look like if the Earth had an orbiting debris ring. Three impact events were evaluated in terms of their long-term effects on climate and we suggest that the late Eocene event is the most likely to have produced at least a moderately opaque orbiting debris ring. The K-T boundary most likely did not experience an impact-generated debris ring even though it was larger than the late Eocene event(s). Although much more remains to be learned about the Neoproterozoic snowball Earth, we suggest that an opaque debris ring could have acted as the trigger to at least one episode of global glaciation through the powerful tropical cooling and attendant high-latitude feedbacks.

Acknowledgements

We thank Karl Wegmann for help in processing the model results and David Gutzler for reviewing an early version of this manuscript. Comments from three anonymous reviewers helped to improve the text. Grants to PJF from the Sandia-University Research Program and NSF (ATM 00-00545) supported this work. This work was funded in part by the Sandia National Laboratories LDRD program (project 10318) and was supported by the United States Department of Energy under Contract DE-AC04-94AL85000. Sandia is a multiprogram laboratory operated by Sandia Corporation, a Lockheed Martin Company, for the U.S. Department of Energy.

References

Alvarez, L.W., W. Alvarez, F. Asaro, and H.V. Michel, 1980, Extraterrestrial cause for the Cretaceous-Tertiary extinction, Science, v. 208, p. 1095-1108.

Barlow, N.G., 1990, Constraints on early events in Martian history as derived from the cratering record, Journal of Geophysical Research, v. 95, p. 14191-14201.

Boslough, M.B.E. and D.A. Crawford, 1997, Shoemaker-Levy 9 and plume-forming collisions on Earth, Annals of the New York Academy of Sciences, v. 822, p. 236-282.

Brahic, A., 1977, Systems of colliding bodies in a gravitational field; numerical simulation of the standard model, Astronomy and Astrophysics, v. 54, p. 895-907.

Brinkhaus, H., J.P. Bujak, J. Smit, G.J.M. Versteegh, and H. Vischer, 1998, Dinoflagellate-based sea surface temperature reconstructions across the Cretaceous-Tertiary boundary, Palaeogeography, Palaeoclimate, Palaeoecology, v. 141, p. 67-83.

Covey, C., S.J. Ghan, J.J. Walton, and P.R. Weissman, 1990, Global environmental effects of impact-generated aerosols; Results from a general circulation model, in Sharpton, V.L., and Ward, P.D., eds., Global catastrophes in Earth history; An

interdisciplinary conference on impacts, volcanism, and mass mortality: Geological Society of America Special Paper 247, p. 263-270.

Covey, C., S.L. Thompson, P.R. Weissman, and M.C. MacCracken, 1994, Global climatic effects of atmospheric dust from an asteroid or comet impact on Earth, Global and Planetary Change, v. 9, p. 263-273.

Crawford, D.A., M.B. Boslough, T.G. Turcano, and A.C. Robinson, 1995, The impact of periodic comet shoemaker-Levy 9 on Jupiter, International Journal of Impact Engineering, v. 17, p. 253-262.

Crowell, J.C., 1983, Ice ages recorded on Gondwanan continents, Transactions of the Geological Society of South Africa, v. 18, p. 238-262.

Cuzzi, J.N., 1983, Planetary ring systems, Reviews of Geophysics and Space Physics, v. 21, p. 173-186.

Cuzzi, J.N. and P.R. Estrada, 1998, Compositional evolution of Saturn's rings due to meteoroid bombardment, Icarus, v. 32, p. 1-35.

D'Hondt, S., M.E.Q. Pilson, H. Sigurdsson, A.K. Hanson, and S. Carey, 1994, Surface-water acidification and extinction at the Cretaceous-Tertiary boundary, Geology, v. 22, p. 983-986.

Endal, A.S., 1981, Evolutional variations of solar luminosity, in Variations of the Solar Constant. NASA Conference Publication 2191, p. 175-183.

Fredricksen, N.O., 1988, Sporomorph biostratigraphy, floral changes, and paleoclimatology, Eocene and Earliest Oligocene of the Eastern Gulf Coast, U.S. Geological Survey Professional Paper, 1448, p. 1-68.

Ganapathy, R., 1982, Evidence for a major meteorite impact on the Earth 34 million years ago: Implication for Eocene extinctions, Science, v. 216, p. 885-886.

Glass, B.P., and P.A. Zwart, 1979, North American tektites in deep-sea drilling project cores from the Caribbean Sea and the Gulf of Mexico, Bulletin of the Geological Society of America, v. 90, p. 595-602.

Hildebrand, A.R., G.T. Penfield, D.A. Kring, M. Pilkington, A. Camargo, Z.S.B. Jacobson, and W.B. Boynton, 1991, Chicxculub Crater: a possible Cretaceous/Tertiary impact crater on the Yucatan Peninsula, Mexico, Geology, v. 19, p. 867-871.

Hoffman, P.F., A.J. Kaufman, G.P. Halverson, and D.P. Schrag, 1998, A Neoproterozoic snowball Earth, Science, v. 281, p. 1342-1346.

Ivany, L.C., W.P. Patterson, and K.C. Lohmann, 2000, Cooler winters as a possible cause of mass extinctions at the Eocene/Oligocene boundary, Nature, v. 407, p. 887-890.

Koeberl, C., W. Poag, W.U. Reimold, and D. Brandt, 1996, Impact origin of the Chesapeake bay structure and the source of the North American tektites, Science, v. 271, p. 1263-1266.

King, E.A., 1980, Late Eocene rings around the Earth? Nature, v. 288, p. 103-104.

Kirschvink, J.L., 1992, Late Proterozoic low-latitude global glaciation: the snowball Earth, in The Proterozoic Biosphere, Schopf, J.W. and Klein, C., eds., Cambridge University Press, New York, p. 51-52.

McLaren, D.J., and W.D. Goodfellow, 1990, Geological and biological consequences of giant impacts, Annual Reviews in Earth and Planetary Sciences, v. 18, p. 123-171.

Melosh, H.J., 1989, Impact Cratering, A Geologic Process, Oxford Monographs on Geology and Geophysics no. 11, New York, Oxford University Press, 245 pp.

Mukhopadhyay, S., K.A. Farley, and A. Montanari, 2001, A short duration of the Cretaceous-Tertiary boundary event: evidence from extraterrestrial Helium-3, Science, v. 291, p. 1952-1955.

Oboh, F.E., C.A. Jaramillo, and L.M. Reeves-Morris, 1996, Late Eocene-Early Oligocene paleofloristic patterns in southern Mississippi and Alabama, US Gulf Coast, Reviews of Paleobotany and Palynology, v. 91, p. 23-34.

O'Keefe, J.A., 1980a, The terminal Eocene event: formation of a ring system around the Earth? Nature, v. 285, p. 309-311.

O'Keefe, J.A., 1980b, Late Eocene rings around the Earth? Reply, Nature, v. 288, p. 104.

O'Keefe, J.A., 1985, The terminal Cretaceous event: circumterrestrial rings of tektite glass particles? Cretaceous Research, v. 6, p. 261-269.

O'Keefe, J.D., and T.J. Ahrens, 1986, Oblique impact: A process for obtaining meteorite samples from other planets, Science, v. 234, p. 346-349.

Pollack, J.B., O.B. Toon, T.P. Ackerman, C.P. McKay, and R.P. Turco, 1983, Environmental effects of an impact-generated dust cloud; implications for the Cretaceous-Tertiary extinctions, Science, v. 219, p. 247-249.

Pollard, D. and S.L. Thompson, 1997, Climate and ice-sheet mass balance at the Last Glacial Maximum from the GENESIS version 2 global climate model, Quaternary Science Reviews, v. 16, p. 841-863.

Prinn, R.G. and B. Fegley, 1987, Bolide impacts, acid rain, and biospheric traumas at the Cretaceous-Tertiary boundary, Earth and Planetary Science Letters, v .83, p. 1-15.

Rampino, M.R., and R.B. Stothers, 1988, Flood basalt volcanism during the last 250 million years, Science, v. 241, p. 663-668.

Raup, D.M., and J.J. Sepkoski, 1986, Periodic extinction of families and genera, Science, v. 231, p. 833-836.

Rea, D.K., M. Leinen, and T.R. Janecek, 1985, Geologic approach to the long-term history of atmospheric circulation, Science, v. 227, p. 721-725.

Rodwell, M.J., and B.J. Hoskins, 2001, Subtropical anticyclones and summer monsoons, Journal of Climate, v. 14, p. 3192-3211.

Schultz, P.H. and D.E. Gault, 1990, Prolonged global catastrophes from oblique impacts, in Sharpton, V.L., and Ward, P.D., eds., Global catastrophes in Earth history; An interdisciplinary conference on impacts, volcanism, and mass mortality: Geological Society of America Special Paper 247, p. 239-261.

Schultz, P.H., M. Zarate, W. Hames, C. Camilión, and J. King, 1998, A 3.3-Ma impact in Argentina and possible consequences, Science, v. 282, p. 2061-2063.

Seyfert, C.K., and L.A. Sirkin, 1979, *Earth History and Plate Tectonics*, New York: Harper & Row.

Shoemaker, E.M., 1983, Asteroid and comet bombardment of the Earth, Annual Review of Earth and Planetary Sciences, v. 11, p. 461-494.

Shoemaker, E., C.S. Shoemaker, and R.F. Wolfe, 1988, Asteroid and comet flux in the neighborhood of the Earth, in Global catastrophes in Earth History; An interdisciplinary conference on impacts, volcanism and mass mortality: Houston, Texas, Lunar and Planetary Institute Contribution 673, p. 174-175.

Sigurdsson, H., S. D'Hondt, and S. Carey, 1992, The impact of the Cretaceous Tertiary bolide on evaporite terrane and generation of major sulfuric-acid aerosol, Earth and Planetary Science Letters, v. 109, p. 543-559.

Spray, J.G., S.P. Kelley, and D.B. Rowley, 1998, Evidence for a late Triassic multiple impact event on Earth, Nature, v. 392, p. 171-173.

Thompson, S.L. and D. Pollard, 1997, Greenland and Antarctic mass balances for present and doubled atmospheric CO2 from the GENESIS version 2 global climate model, Journal of Climate, v. 8, p. 1104-1121.

Toon, O.B., K. Zahnle, D. Morrison, R.P. Turco, and C. Covey, 1997, Environmental perturbations caused by the impacts of asteroids and comets, Reviews of Geophysics, v. 35, p. 41-78.

Toon, O.B., J.B. Pollack, T.P. Ackerman, R.P. Turco, and C.P. McKay, 1982, Evolution of an impact-generated dust cloud and its effects on the atmosphere, in Silver, L.T. and P.H. Schulz, eds., Geological implications of impacts of large asteroids and comets on the Earth, Geological Society of America Special Paper 190, p. 187-200.

Vonhof, H.B., and J. Smit, 1999, Late Eocene microkrystites at Maud Rise (Ocean Drilling Project Hole 689B; Southern Ocean) suggest a global extension of the approximately 35.5 Ma Pacific impact ejecta strewn field, Meteoritics & Planetary Science, v. 34, p. 747-755.

Vonhof, H.B., J. Smit, H. Brinkhuis, A. Montanari, and A.J. Nederbragt, 2000, Global cooling accelerated by early late Eocene impacts? Geology, v. 28, p. 687-690.

Wei, W.C., 1995, How many impact-generated microspherule layers in the upper Eocene? Palaeogeography, Palaeoclimatology, Palaeoecology, v. 114, p. 101-110.

Williams, G.E., 1994, Acraman: A major impact structure from the Neoproterozoic of Australia, in Dressler, B.O., Grieve, R.A.F., and Sharpton, V.L., eds., Large

Meteorite Impacts and Planetary Evolution: Boulder, Colorado, Geological Society of America Special Paper 293, p. 209-224.

Wolfe, J.A., 1978, A paleobotanical interpretation of Tertiary climates in the Northern Hemisphere, American Scientist, v. 66, p. 694-703.

Zachos, J.D., L.D. Stott, and K.C. Lohmann, 1994, Evolution of early Cenozoic marine temperatures, Paleoceanography, v. 9, p. 353-387.

Zachos, J.C., J.R. Breza, and S.W. Wise, 1992, Early Oligocene ice-sheet expansion on Antarctica: Stable isotope and sedimentological evidence from Kerguelen Plateau, southern Indian Ocean, Geology, v. 20, p. 569-573.

Figure Captions

Figure 1. The seasonal migration of a subtropical insolation shadow caused by an equatorial debris ring in orbit around the Earth.

Figure 2. Solar insolation incident on a unit horizontal surface at the top of the atmosphere, modified by an equatorial debris ring in orbit. Area in black shows the extent of the ring shadow. Units in W/m^2.

Figure 3. Model predicted surface temperature for the ring shadow simulation ($5^{o}C$ contour interval): (a) June-July-August (JJA) and (b) December-January-February (DJF). Latitudinal ranges of the ring shadow at the solstices are shown as black boxes to the right.

Figure 4. Zonally averaged surface temperature for two simulations. The solid line is the control experiment and the dashed line is the ring shadow experiment: (a) JJA and (b) DJF. The absolute temperature differences for both seasons are plotted below.

Figure 5. Average surface temperature differences (control minus ring shadow): (a) JJA and (b) DJF. Variable contour interval, see legend. Negative difference contours are dashed. Latitudinal ranges of the ring shadow at the solstices are shown as black boxes to the right.

Figure 6. Model predicted sea-level pressure (5 mb contour interval) for the ring simulation: (a) JJA and (b) DJF. Positions of highs and lows marked with H and L respectively. Latitudinal ranges of the ring shadow at the solstices are shown as black boxes to the right.

Figure 7. Average sea-level pressure differences (control minus ring shadow): (a) JJA and (b) DJF. Contour interval is 2 mb. Negative differences (dashed lines) indicate higher pressure in the ring simulation and positive differences (solid lines) indicate lower pressure in the ring simulation relative to the control simulation.

Figure 8. Model predicted surface winds for the ring simulation: (a) JJA and (b) DJF. Maximum wind vector is given for each season in m/s. Latitudinal ranges of the ring shadow at the solstices are shown as black boxes to the right.

Figure 9. Model predicted meridional cross section of longitudinally averaged zonal winds (5 m/s contour interval) for the ring simulation: (a) July and (b) January.

Figure 10. Model predicted precipitation rates (contour interval of 1 mm/day) for the ring simulation: (a) JJA and (b) DJF. Areas of precipitation greater than 6 mm/day are shaded.

Figure 11. Zonally averaged precipitation rates for two simulations. The solid line is the control experiment and the dashed line is the ring shadow experiment: (a) JJA and (b) DJF.

Figure 12. Average precipitation rate differences (control minus ring shadow): (a) JJA and (b) DJF. Contour interval of 1 mm/day, negative differences (wetter areas in the ring simulation relative to the control) are dashed lines. Areas of difference greater than 4 mm/day are shaded as shown in legend. Zero contour line is the heavier black line. Latitudinal ranges of the ring shadow at the solstices are shown as black boxes to the right.

Figure 13. Zonally averaged evaporation rates for the control (solid line) and ring (dashed line) simulations: (a) JJA and (b) DJF. The absolute differences (mm/day) between the two are plotted also (heavy black line). Latitudinal ranges of the ring shadow at the solstices are shown as black boxes to the right.

Figure 14. Model predicted snow cover and sea-ice distribution for the ring simulation: (a) JJA and (b) DJF. Snow thickness contour interval is 10 cm. Sea-ice margin is equivalent to the 10 cm contour over ocean areas.

Figure 1

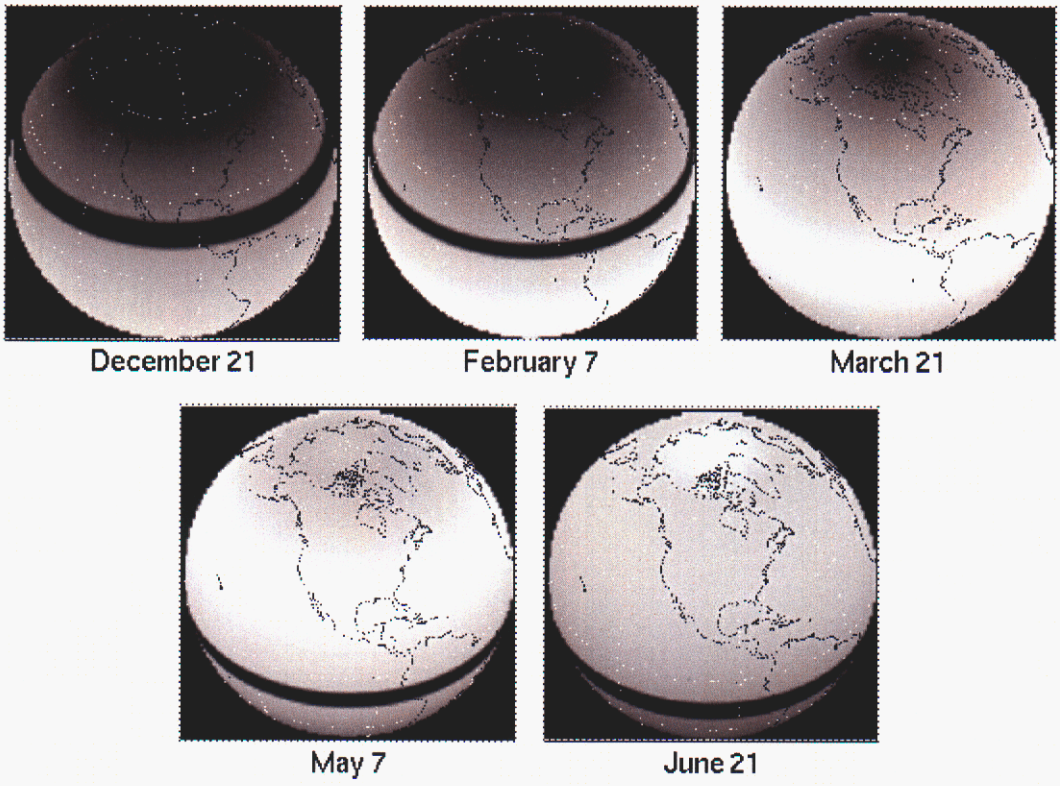

Figure 2

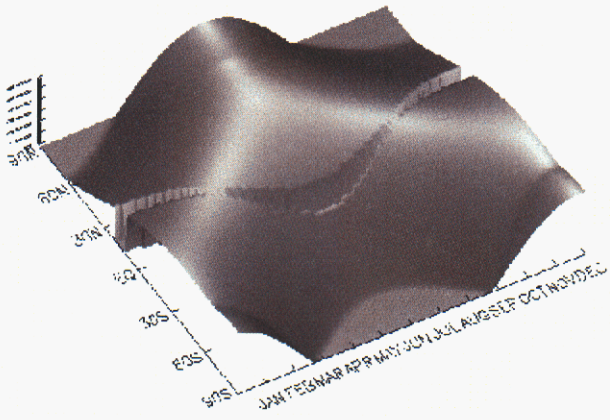
90N
60N
30N
EQ
30S
60S
90S
JAN FEB MAR APR MAY JUN JUL AUG SEP OCT NOV DEC

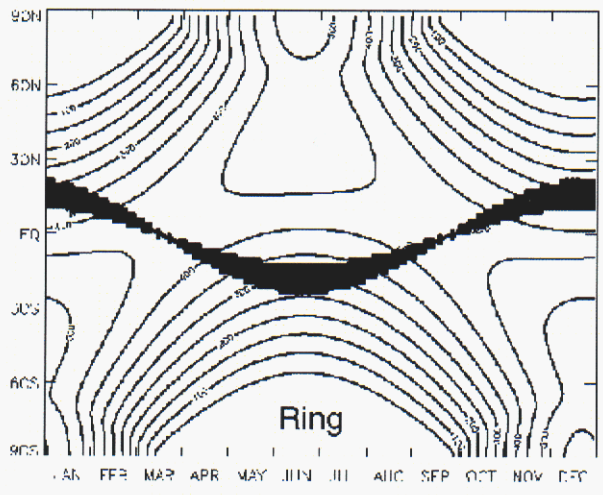
90N
60N
30N
EQ
30S
60S
90S
Ring
JAN FEB MAR APR MAY JUN JUL AUG SEP OCT NOV DEC

Figure 3

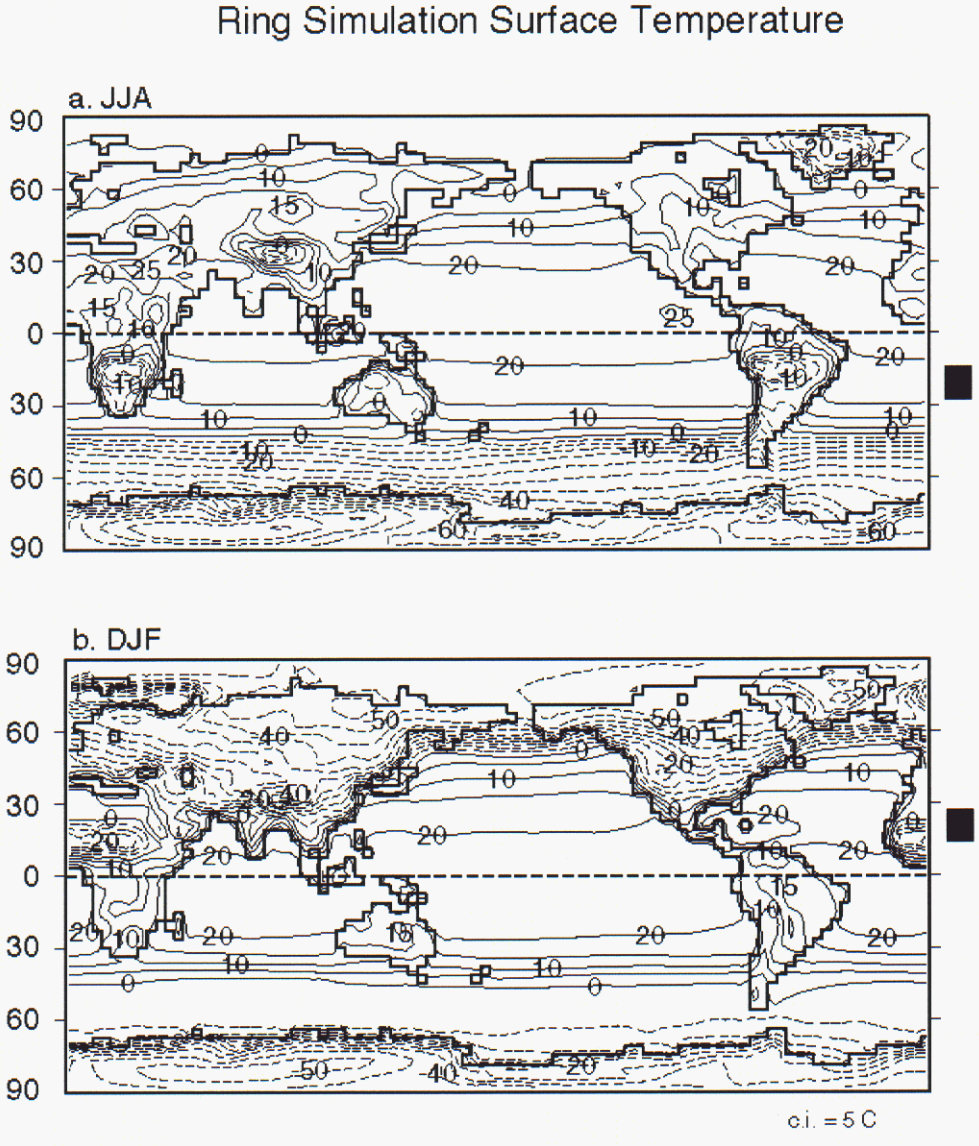
Ring Simulation Surface Temperature
a. JJA
b. DJF
90
60
30
0
30
60
90
c.i. = 5 C

Figure 4

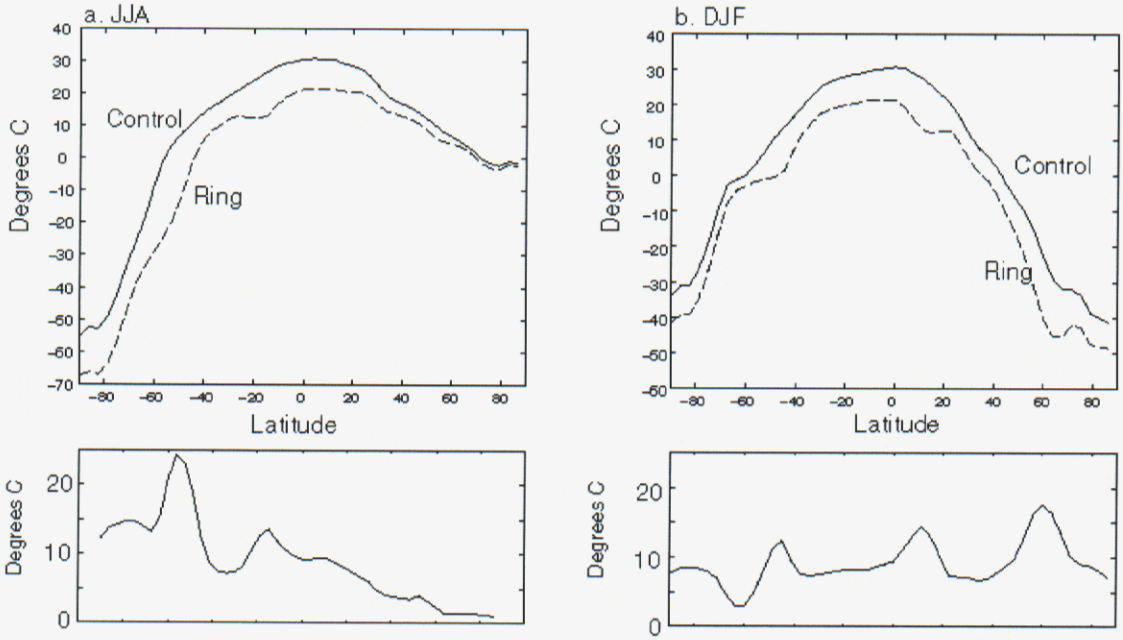
Control vs. Ring Surface Temperature
a. JJA
Control
Ring
Degrees C
Latitude
b. DJF
Control
Ring
Degrees C
Latitude

Figure 5

Surface Temperature Difference

Control minus Ring

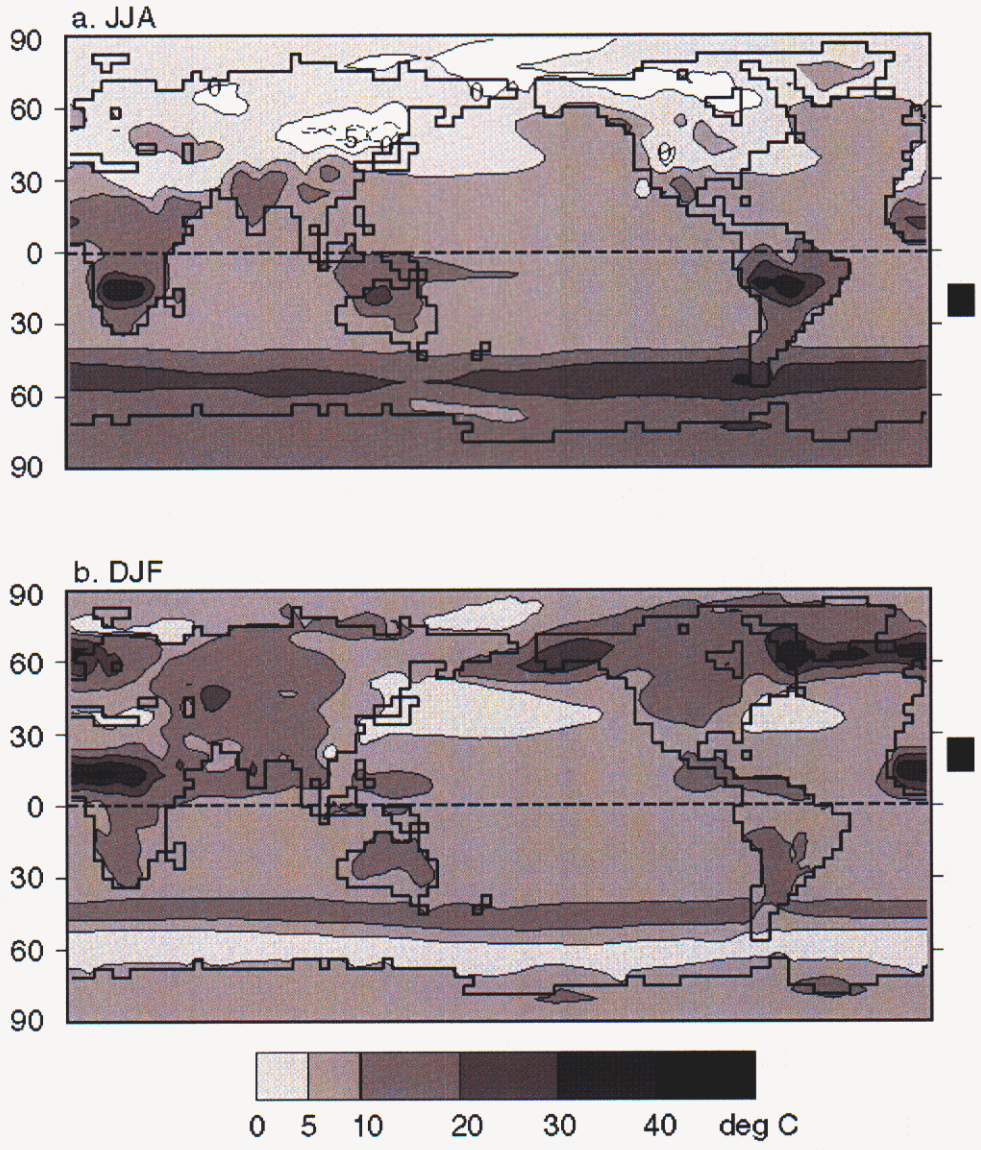

Figure 6

Ring Simulation Sea-Level Pressure

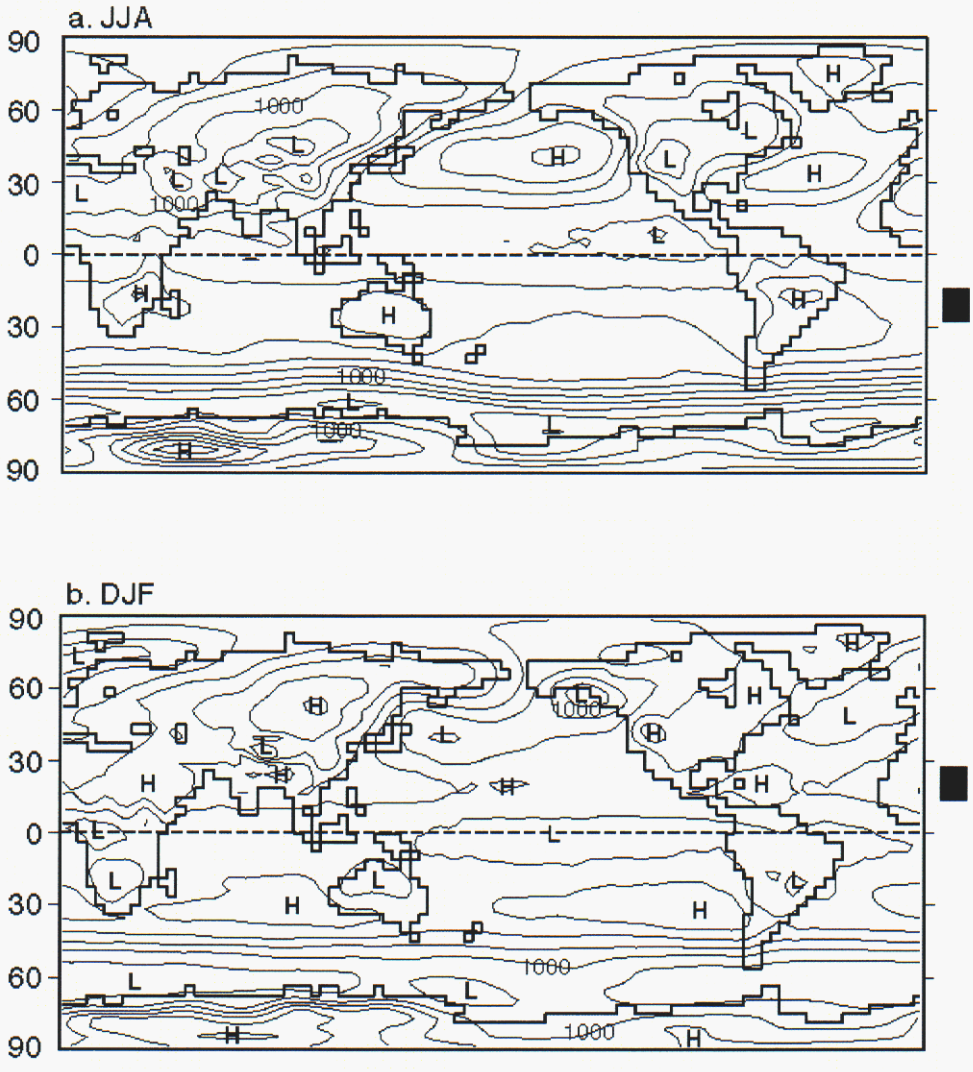

Figure 7

Sea-Level Pressure Difference

Control minus Ring

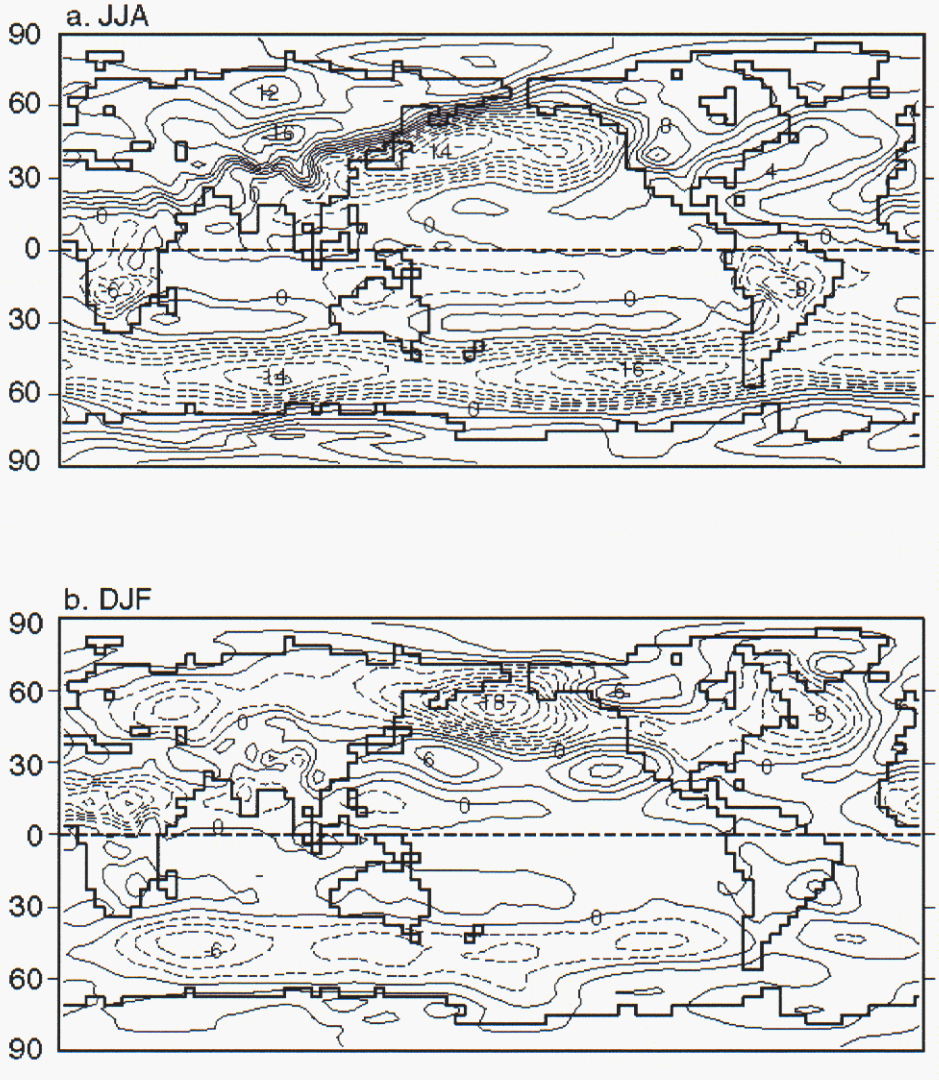

contour interval = 2 mb

Figure 8

Ring Simulation Surface Winds

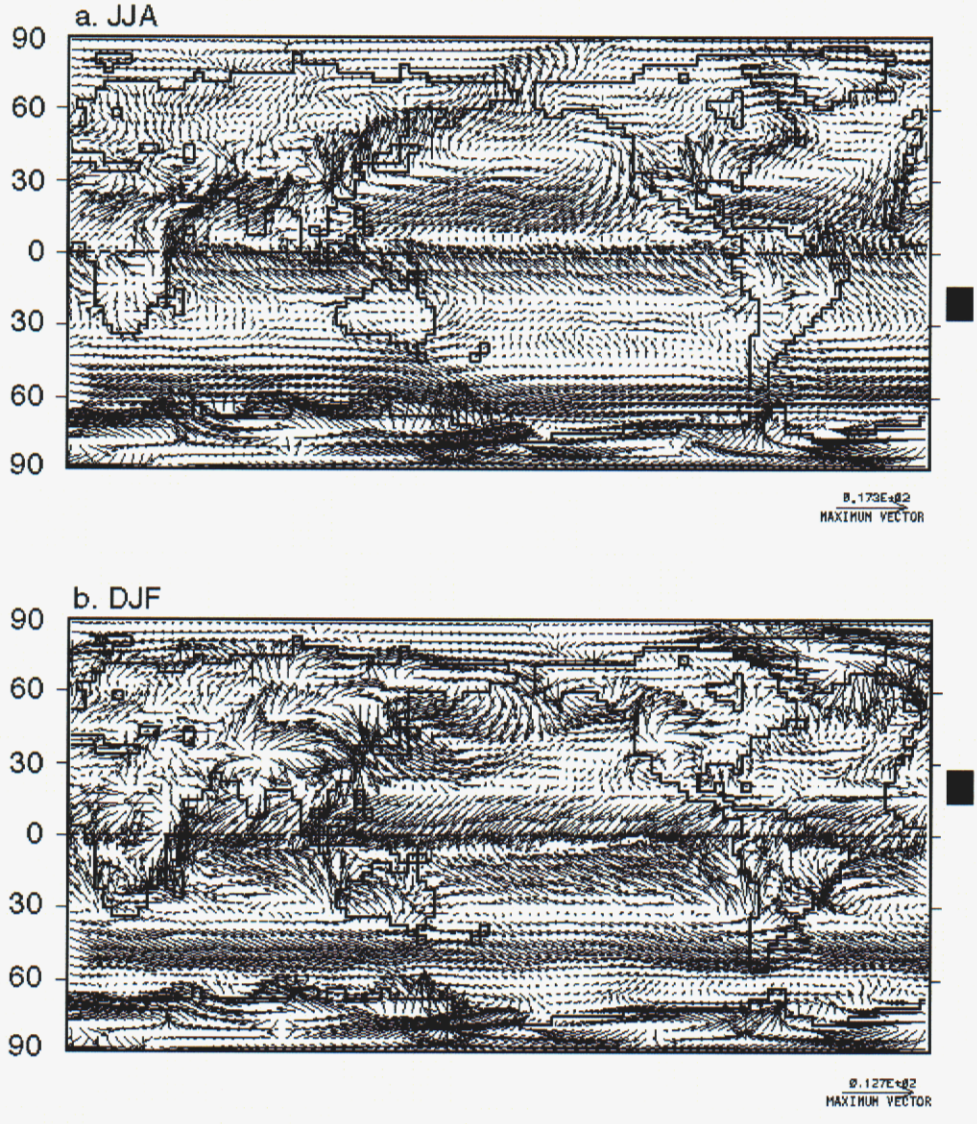

Figure 9

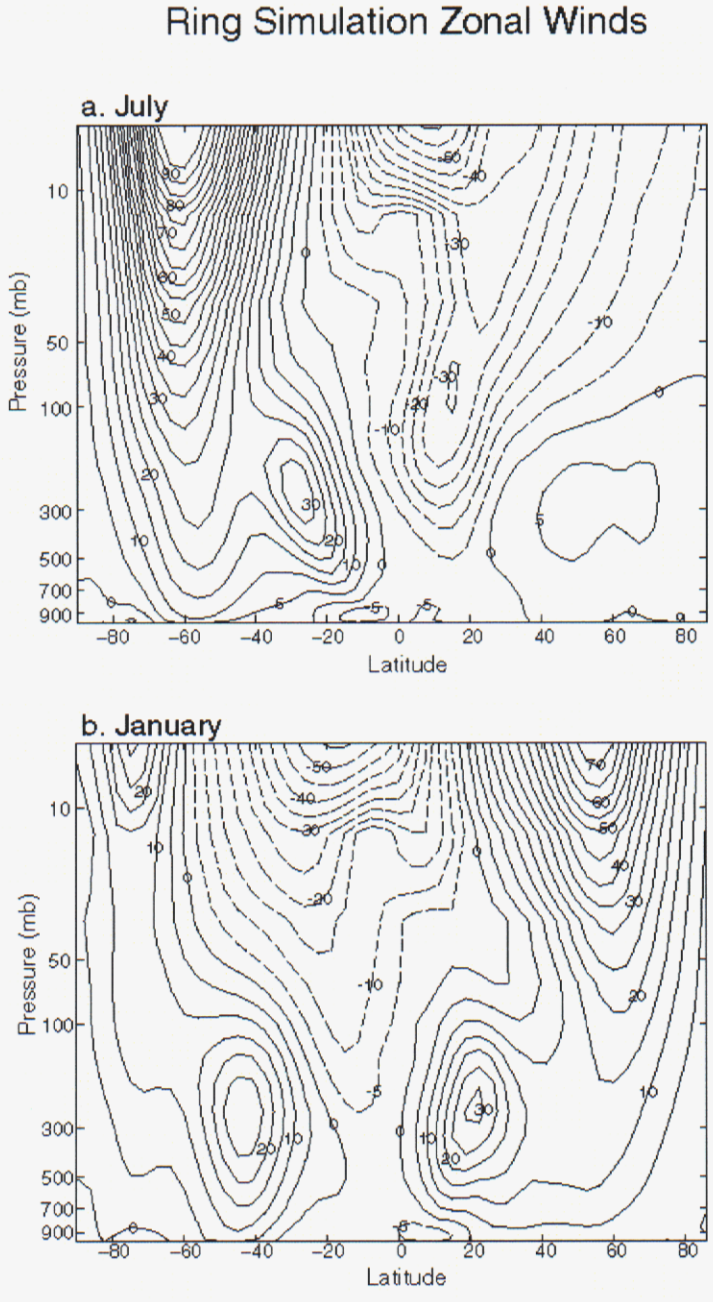
Ring Simulation Zonal Winds
a. July
Pressure (mb)
10
50
100
300
500
700
900
−80 −60 −40 −20 0 20 40 60 80
Latitude
b. January
Pressure (mb)
10
50
100
300
500
700
900
−80 −60 −40 −20 0 20 40 60 80
Latitude

Figure 10

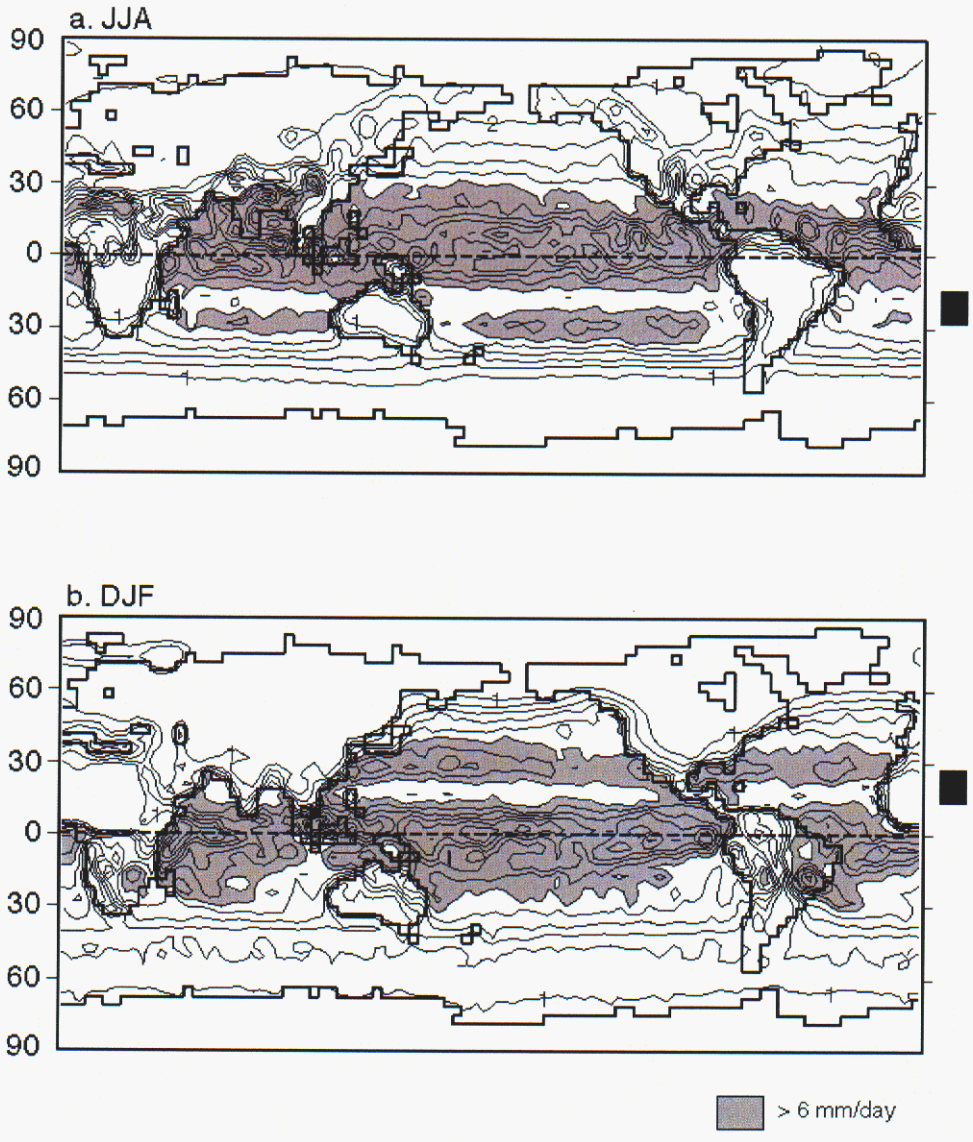
Ring Simulation Precipitation
a. JJA
90
60
30
0
30
60
90
b. DJF
90
60
30
0
30
60
90
> 6 mm/day

Figure 11

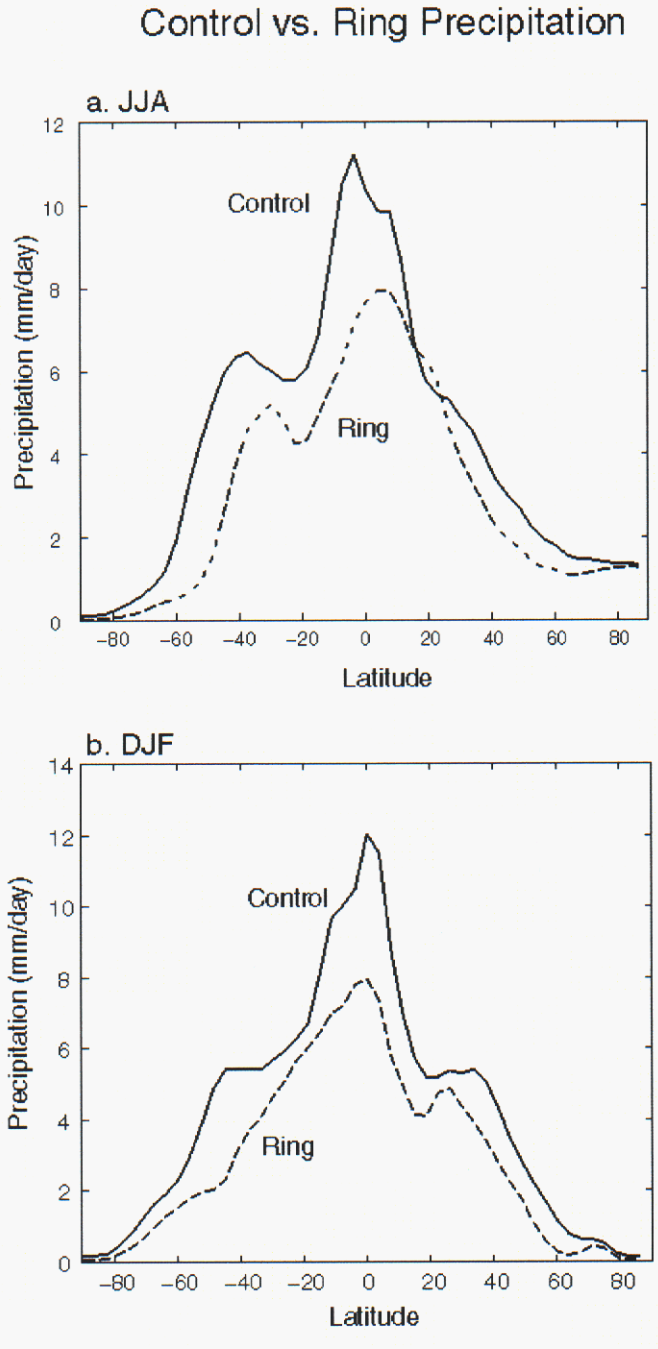
Control vs. Ring Precipitation
a. JJA
Precipitation (mm/day)
Control
Ring
Latitude
b. DJF
Precipitation (mm/day)
Control
Ring
Latitude

Figure 12

Precipitation Difference

Control minus Ring

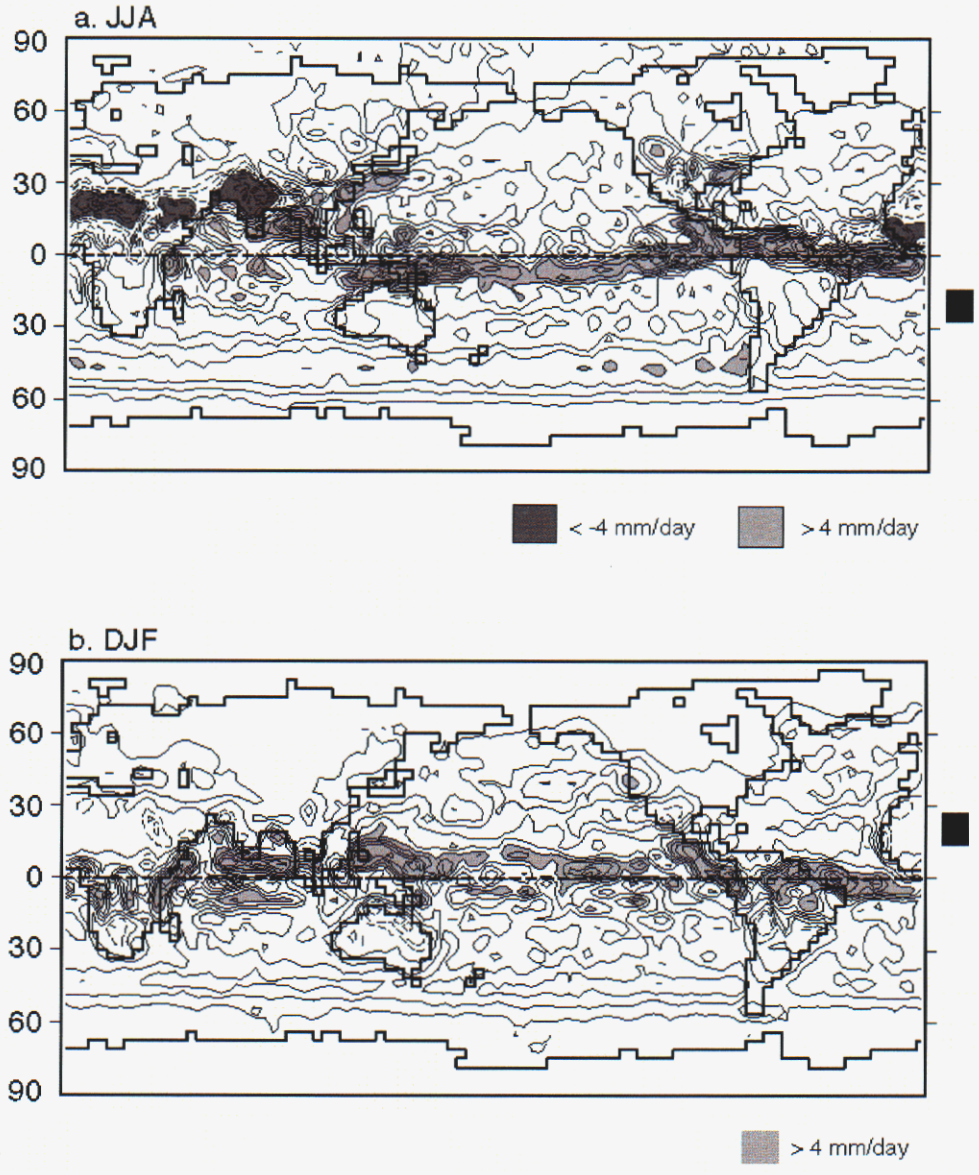

Figure 13

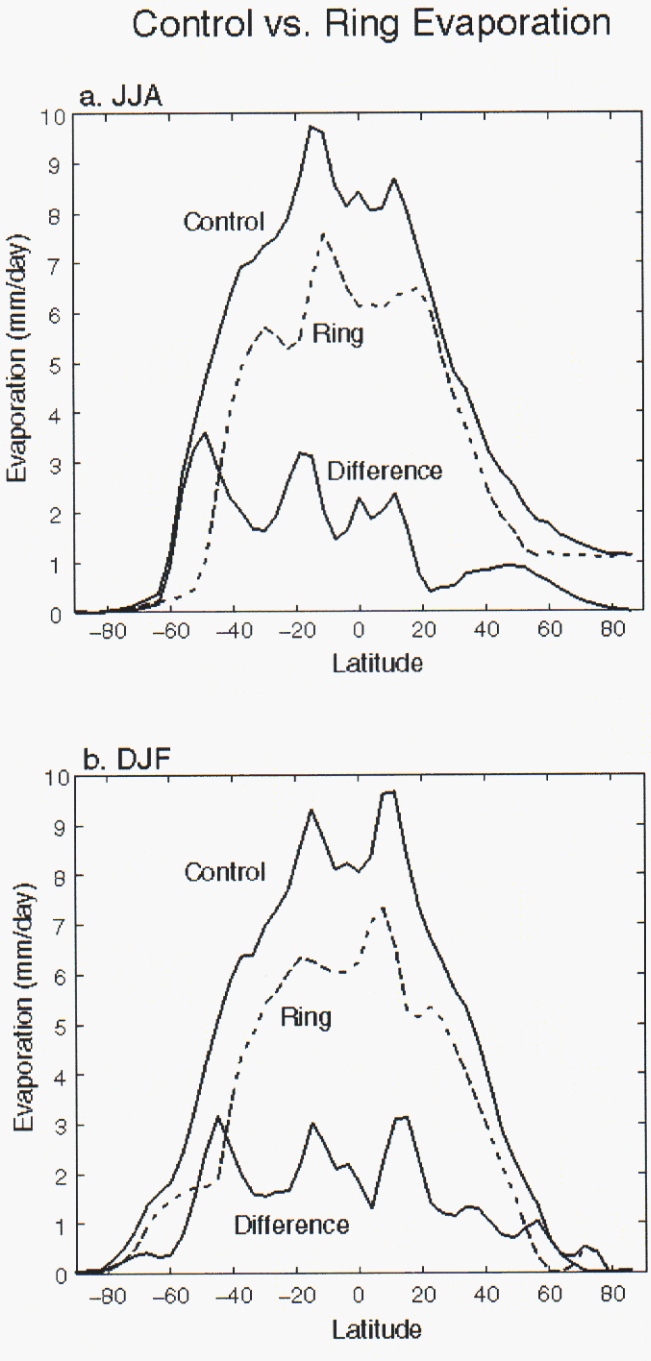
Control vs. Ring Evaporation
a. JJA
Evaporation (mm/day)
Control
Ring
Difference
Latitude
b. DJF
Evaporation (mm/day)
Control
Ring
Difference
Latitude

Figure 14

Ring Simulation Snowcover and Sea-Ice Extent

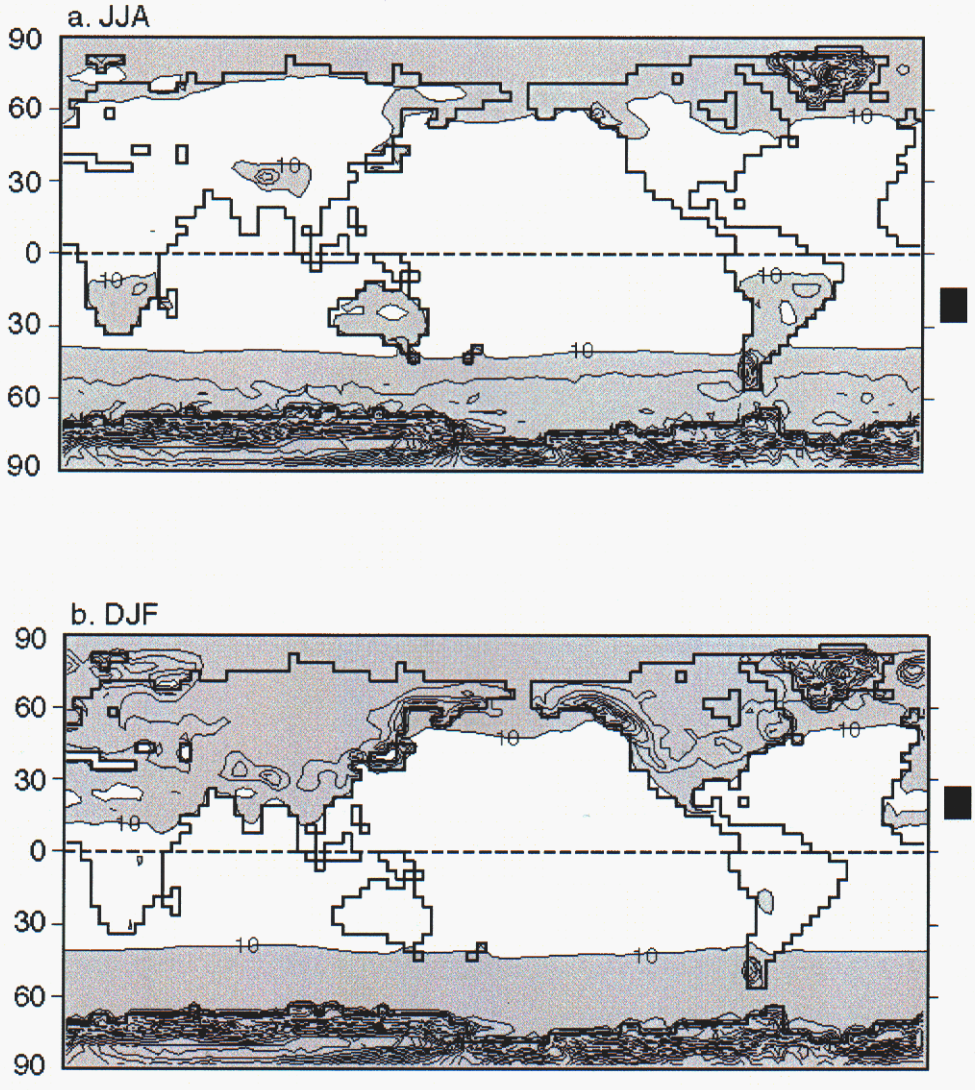

Appendix B

Boslough, M.B.E. (2001), "Impact-Induced Climate Change due to an Orbiting Debris Ring," 20th Annual Int. Space Dev. Conf, ASCE, SAND2001-1710C.

IMPACT-INDUCED CLIMATE CHANGE DUE TO AN ORBITING DEBRIS RING

Mark B. E. Boslough
Sandia National Laboratories, Albuquerque, New Mexico 87185-0318

International Space Development Conference: 2001
Albuquerque, New Mexico
May 24-28, 2001

IMPACT-INDUCED CLIMATE CHANGE DUE TO AN ORBITING DEBRIS RING

Mark B. E. Boslough
Sandia National Laboratories, Albuquerque, New Mexico 87185-0318

Abstract

The effect of time-dependent incoming solar radiation (insolation) losses due to the shadow of an opaque orbiting ring around the Earth is addressed using a modified version of the atmospheric general circulation model GENESIS. Twelve simulations were run using three different sets of orbital parameters; three without rings, and nine with two different ring models. One set of simulations was performed using two different initializations as a stability and convergence check. The three sets of orbital parameters were chosen to simulate glaciation-favoring and glaciation-inhibiting conditions in the northern hemisphere, as well as current conditions. The objective was to address the question of whether a impact-generated ring could amplify or diminish certain Milankovich periods in a way that might be evident in the geologic record.

Introduction

Many ideas have been proposed for the K/T boundary extinction, including production of massive amounts of nitrogen oxides by shock-induced chemical reactions in the atmosphere, shock devolatilization of carbonate and anhydrite target rocks producing carbon dioxide and sulfur compounds, and production of a long-lived opaque aerosol layer from impact ejecta with smoke from global firestorms. Some combination of these effects would result in a large transient change in atmospheric chemistry, insolation, albedo, and long-wave radiative properties. Alvarez et al. [1] suggested that the diameter of the impactor was about 10 km based on the global quantity of iridium in the K/T boundary. The best estimate of the projectile size has not changed significantly in the years since Chicxulub has been discovered and characterized. The K/T boundary undoubtedly represents the largest impact event of the last hundred million years. However, the significance of this event has more to do with its relative recency and the particular fauna that disappeared that with its uniqueness over geologic time.

Shoemaker [2] estimated that impacts of K/T size (releasing on the order of 10^8 Mt of kinetic energy) take place on Earth with a mean recurrence interval of about 10^8 years. That rate implies that there has been a score of K/T class impacts since the beginning of the Proterozoic (about 2.5 billion years ago). Moreover, Shoemaker's power-law distribution of impact events means that since the termination of the Mesozoic Period by the K/T event, there have been ten impacts of about 10^7 Mt, a hundred events of 10^6 Mt (roughly the size of all Shoemaker-Levy 9 fragments

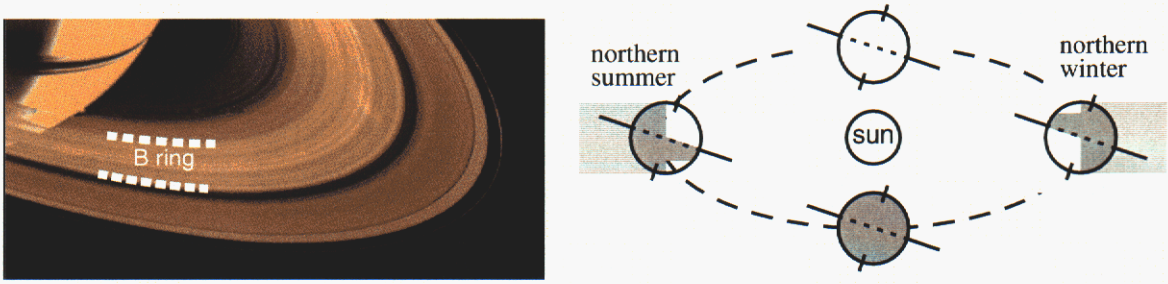

Figure 1. Voyager spacecraft image of Saturn showing the opaque B-ring and its shadow on the planet's cloud tops (left), seasonal effect of equatorial ring on insolation (right).

combined), and a thousand impacts of 10^5 Mt (about the size of the impact that asteroid 1997 XF_{11} would have made, if it had been on an Earth-intersecting path).

If climate is indeed sensitive to such events, then it is virtually certain that many of these impacts left signatures in the geologic record besides holes in the ground. The work presented here suggests that the sedimentary record might contain evidence for impacts beyond ejecta layers, and that both transient and long-term impact-generated climate effects might be seen in sedimentary rocks due to the formation of a transient debris ring in Earth orbit. Modeling of climate change by various mechanisms can provide insight to help interpret the geologic evidence.

The Geologic Record

The most obvious sedimentary record of an impact is the clay layer left by the ejecta from the K/T event. This layer was first associated with an impact because of the high concentration of platinum-group elements discovered in the clay from the K/T boundary at Gubbio, Italy. Subsequently, other evidence for impact was found in the layer, including shocked mineral grains and spherules. These observations were direct evidence for an impact, because the materials were derived from the impacting body or from the impact event itself.

One can look at the larger stratigraphic sequence and also note that there was a climatic shift at the K/T boundary. The Cretaceous and Tertiary sedimentary cycles are dominated by the approximately 20 thousand year (ky) period associated with precession. Below the boundary these are bundled into 100 ky eccentricity cycles, but that is no longer true above the boundary. This observation implies that the impact event not only caused a the large transient climate change responsible for the extinction, but that it somehow changed in the planet's sensitivity to orbital forcing for hundreds of thousands of years afterward.

Another abrupt change in sensitivity to orbital forcing took place 700,000 years ago, at virtually the same time as the Australasian tektite-forming event for which an impact structure has not yet been discovered. In this mid-Pleistocene case, obliquity-dominated (40 ky) cycles were replaced by eccentricity-dominated (100 ky) cycles which continue to persist (the "mid-Pleistocene transition").

Possible Mechanisms

Most of the proposed mechanisms for climate change caused by impacts are related to atmospheric chemistry and aerosols, and such impact-induced climate changes are usually thought to be transient, with an eventual return to pre-impact conditions. However, the changes in Milankovich sensitivity suggest that there are longer-term effects that need to be understood. Few hypotheses have been proposed to explain the shifts in orbital forcing at the end of the Mesozoic and in the mid-Pleistocene. The mechanism to be explored in this paper is the generation by a large impact of a ring that encircles the equatorial region of the Earth. The global extent of iridium, spherules, and shocked quartz at the K/T boundary clearly demonstrate that material is ejected at orbital velocities. A purely ballistic ejection that does not involve atmospheric interactions would not allow such particles to remain in orbit, and they would reenter the atmosphere and impact within one orbital period. However, atmospheric interactions are increasingly being recognized as an important component of terrestrial impact physics, and this could possibly provide the conditions that would lead to orbital trapping of debris through hydrodynamic forces within an expanding plume that alters the trajectories of some particles in such a way that they do not re-enter the atmosphere.

Discussion

Until more simulations and analyses can be done, the explanation for ring-enhanced high latitude northern hemisphere summer temperatures can only be speculative. The implications for late Pliocene to mid Pleistocene glacial-interglacial cycles are the most intriguing. The ocean sediment $\delta^{18}O$ proxy record for ice abundance during this span of time [5] shows a strong 40-ky signal up until about 700 ky before present. At that time there was a switch to a 100-ky-dominated oscillation with much higher amplitude. The 40-ky period is almost certainly associated with obliquity forcing, which implies that the Earth's climate system went through a major transformation 700 ky ago that decreased its sensitivity to obliquity forcing. One possibility is that Earth had a ring system prior to that time, and its disappearance resulted in the observed climate transition.

This suggestion immediately leads to a whole host of questions. How did the ring form? What was it made of an how much mass would be required? How did it disappear? Recent 3D computational simulations (David Crawford, personal communication) have shown that for a oblique asteroid impact, with an entry angle of less than 15^{o} , the entire asteroidal mass--as well as significant quantities of ocean water and crustal rock--can be ejected at velocities approaching escape velocity. It is reasonable to expect that some of this material would be captured into a stable set of orbits by a combination of atmospheric interactions, hydrodynamic forces, and interparticle interactions. The surface area of a B-like ring scaled to Earth's radius is about $1.8x10^{18}$ cm^2. About 10^{17} g of mm-size particles (assuming a density of about 3 g/cm^3) would be required for the ring to have an optical depth of unity, which would be nearly opaque for the range of solar declination angles experienced. A 10 km-diameter asteroid, about the same as the estimated size of the K/T impactor, would be required if its entire mass went into the ring. Micron-size particles, typical for Jupiter's rings, would required the mass equivalent of a 1 km asteroid. However, such small particles are probably unrealistic because Poynting-Robertson drag (deflections from photon interactions) and plasma drag with the Earth's magnetospheric plasma would severely limit the lifetime of such a ring. The Saturnian and Uranian ring system particles are estimated to be centimeters to meters in diameter. This would require much more mass for significant opacity. Nevertheless, if the enhancement of obliquity forcing is as strong as the climate simulations suggest, a ring with modest opacity might lead to significant amplification.

It is possible that an existing ring system could be sporadically replenished by random asteroid or comet collisions. There were several significant impacts during the Pliocene and Pleistocene. One of the largest was the Eltanin event in the southeast Pacific, about 2.3 million years ago. The estimated asteroid diameter is 0.5 km, but it could have been as large as 2.0 km if the impact angle was oblique ($<15^{o}$ entry angle). Kyte et al. [6] believe that the time of the impact is unresolvable from the onset time of Northern Hemisphere glaciation (between 2.5 and 3.0 million years ago) and suggest that this could have been caused by the injection of at least $2x10^{15}$ g of seawater into the atmosphere, which saturated the atmosphere and generated global high-altitude clouds, ultimately leading to lower temperatures and more continental area covered by snow. The time of the Eltanin impact also seems to correlate with a shift in the marine oxygen isotope record that is consistent with several periods of much greater than usual ice cover at that time. Another potential ring-replenishing event could be the impact associated with the formation of the Lake Bosumtwi crater in Ghana about 1.1 million years ago.

Perhaps even more provocative is the possibility that such a ring did not gradually erode but disrupted catastrophically about 760,000 years ago, resulting in the Australasian tektite strewnfield--which has no known associated impact structure--and accounting for the sudden departure from strong obliquity period dependence of ice quantity evident in the oxygen isotope record. The

Muong-Nong Tektites of southeast Asia have been particularly difficult to explain because they appear to have formed from vitrification of soil over an extensive area, which seems inconsistent with a single impact. Boslough and Crawford [7] suggested that a swarm of impactors simultaneously entered the atmosphere over a large region, generating a collective atmospheric plume that collapsed and heated the atmosphere. This in turn radiatively melted the soil, which was rapidly quenched by heat conduction into the cooler substrate. The weakest part of this hypothesis has been the lack of an explanation for a source of the necessary tightly-correlated swarm of debris. This would be resolved if the impactors were from a collapsing ring, but the revised hypothesis requires an explanation for why such a collapse would be sudden.

The Goldreich-Tremaine [8] model for ring stability invokes the existence of shepherd satellites. An inner satellite moves in a faster, lower orbit, and continuously gives up some of its orbital energy to ring particles, forcing them into higher orbits. On the other side, an outer slower satellite captures energy from the ring particles thereby pushing them into a lower orbit. If both shepherds are present, then a narrowly "collimated" ring can be stable. However, such a ring has a limited lifetime, with the whole system loses energy due to various drag forces, and the inner shepherd's orbit will eventually decay until it enters Earth's atmosphere. This would be expected to cause a loss of ring focusing from the inside, leading to an instability with eventual dissipation of the ring. However, because of the shepherd entry event itself, the rest of the ring can collapse within one orbit due to the generation of an atmospheric plume [7]. When the shepherd deposits its kinetic energy into the Earth's atmosphere, a Shoemaker-Levy-like plume would be ejected hundreds of kilometers into space, directly into the path of the ring particles. The ring particles that collide with the plume would lose their kinetic energy and vaporize, increasing the plume's mass and internal energy. Because the ballistic trajectory would keep the plume aloft long enough for a significant fraction of the ring to accrete, the plume's growth would be a runaway process with mass and energy being added at a faster rate than it dissipates, catastrophically consuming the entire ring and disrupting the Earth's atmosphere.

This phenomenon is extremely speculative and has never been modeled, but there are other lines of evidence that might provide support. The Australasian strewn field spans the equator, and the Muong-Nong tektites are at a latitude that would be within the range of a ring in the lunar orbital plane. Generation of objects large enough to be shepherd moons is difficult by impact, but not out of the question. Schultz and Gault [9] demonstrated that fragments up to 10% of the impactor diameter can be placed into very eccentric orbits for oblique impact angles of less than 15^{o}. The K/T boundary, which might be associated with another ring-producing impact, does not have the sharp iridium spike right at the boundary, as one might expect for a single layer of ejecta derived from an extraterrestrial object. Instead, the iridium-rich material is found only at he top of a complex K/T sequence, suggesting that there was a re-accretion of material ejected into orbit [10]. If speculations about the existence of impact-generated planetary rings have any merit, then one would expect to eventually find more compelling evidence in the geologic record.

Conclusions

Comparison of the results of climate simulations for a ringless and ringed Earth reveal that the winter hemisphere is much colder for a ringed Earth. This would be expected because in the winter hemisphere, insolation is reduced by an equatorial ring. At northern mid-to-high latitudes, the winter temperatures are as much as 9^{o}C colder in January in North America. The amount of winter cooling shows no clear trends; it is roughly the same for all orbital conditions examined. However, the summer high-latitude insolation varies with obliquity in an unexpected way for a ringed

Earth. In Canada and Siberia, the high obliquity July temperatures are as much as 10 to 15°C warmer for a ringed planet. This increase is compensated by a decrease at lower latitudes. For the other orbital conditions, the same high-latitude locations are within a few degrees. This result is significant because high latitude summer temperatures control the formation of ice sheets.

The high northern latitude summer temperature increases for a ringed Earth are difficult to explain without further work, but if the result is true it means that the existence of rings would amplify the greenhouse/icehouse cycle with a 40,000 year period. Combining this result with the $\delta^{18}O$ proxy record for ice abundance leads to the speculation that Earth had a ring system during the late Pliocene and early Pleistocene, and that it eroded and disappeared about 700,000 years ago, approximately coincident with the formation of the Australasian tektites. This suggestion is tentative, and currently has a only a weak foundation in both impact physics and climatological modeling. No modeling of ring dynamics has been done to determine the stability and lifetime of a hypothetical terrestrial ring system, how it would form, evolve, decay, and disappear. The physics of ring-forming impacts, orbital dynamics of such rings, and climatology of a ringed Earth are all fertile areas for more computational research to be guided by this working hypothesis.

References

1. Alvarez, L.W., W. Alvarez, F. Asaro, and H.V. Michel (1980), "Extraterrestrial cause of the Cretaceous/Tertiary extinction", *Science* **208**: 1095-1108.
2. Shoemaker, E.M. (1983), "Asteroid and comet bombardment of the Earth", *Ann. Rev. Earth Planet. Sci.* **11**: 461-494.
3. Pollard, D., and S.L.Thompson (1992), "Users' guide to the GENESIS global climate model version 2.0", National Center for Atmospheric Research, Boulder, Colorado, 58 pp.
4. Fawcett, P.J. and M.B.E. Boslough (2001), "Climatic effects of an impact induced equatorial debris ring", *J. Geophys. Res,* submitted.
5. Raymo, M.E., W.F. Ruddiman, N.J. Shackleton, and D.W. Oppo (1990), "Evolution of Atlantic-Pacific δC^{13} gradients over the last 2.5 m.y.", *Earth. Planet. Sci. Lett.* **97**: 353-368.
6. Kyte, F.T., L. Zhou, and J.T. Wasson (1988), "New evidence on the size and possible effects of a late pliocene oceanic asteroid impact", *Science* **241**: 63-65.
7. Boslough, M.B.E. and D.A. Crawford (1997), "Shoemaker-Levy 9 and plume-forming collisions on Earth", *Annals of the New York Acad of Sciences* **822**: 236-282.
8. Goldreich, P. and S. Tremaine (1982),"The dynamics of planetary rings", *Ann. Rev. Astron Astrophys.* **20**: 249-283.
9. Schultz, P. H. and D.E. Gault (1989), "Protracted global catastrophes from oblique impacts", *Lunar and Planet. Sci. Conf.* **20**: 970-971.
10. Rocchia, R., Robin, E., Froget, L, and Gayraud, J. (1996), "Stratigraphic distribution of extraterrestrial markers at the Cretaceous-Tertiary boundary in the Gulf of Mexico area: Implications for the temporal complexity of the event", *GSA Special Paper* **307**: 279-286.

Acknowledgments

This work was funded in part by the Sandia National Laboratories LDRD program (project 10318) and was supported by the United States Department of Energy under Contract DE-AC04-94AL85000. Sandia is a multiprogram laboratory operated by Sandia Corporation, a Lockheed Martin Company, for the United States Department of Energy. Peter Fawcett, Dave Gutzler, and Maya Elrick generously provided comments and ideas.

DISTRIBUTION

MS 0310 A. Backer, 9212
MS 0318 M.B.E. Boslough, 9212 (20)
MS 0318 K. Boyack, 9212
MS 0196 C. Churchwell, 9212
MS 0318 G. S. Davidson, 9212
MS 9951 J-L. Faulon, 9212
MS 0316 L. Frink, 9212
MS 0196 S. Martin, 9212
MS 0196 E. May, 9212
MS 1109 R. Pryor, 9212
MS 0316 S. Rempe, 9212
MS 0316 M.D. Rintoul, 9212
MS 0321 W. Camp, 9200
MS 0612 Review and Approval Desk, 9612
MS 0899 Technical Library, 9616 (2)
MS 9018 Central Technical Files, 8945-1